January 2002 • NREL/SR-500-30117

Subcontractor Report

Laboratory Testing of Drivetrain Component Efficiencies for Constant-Speed and Variable-Speed Wind Turbines

November 4, 1997—November 3, 2000

Global Energy Concepts, L.L.C.
Kirkland, Washington

National Renewable Energy Laboratory

1617 Cole Boulevard
Golden, Colorado 80401-3393

NREL is a U.S. Department of Energy Laboratory
Operated by Midwest Research Institute • Battelle • Bechtel

Contract No. DE-AC36-99-GO10337

January 2002 • NREL/SR-500-30117

Laboratory Testing of Drivetrain Component Efficiencies for Constant-Speed and Variable-Speed Wind Turbines

November 4, 1997—November 3, 2000

Global Energy Concepts, L.L.C.
Kirkland, Washington

NREL Technical Monitor: Paul Migliore

Prepared under Subcontract No. TAM-8-17228-01

National Renewable Energy Laboratory

1617 Cole Boulevard
Golden, Colorado 80401-3393

NREL is a U.S. Department of Energy Laboratory
Operated by Midwest Research Institute • Battelle • Bechtel

Contract No. DE-AC36-99-GO10337

NOTICE

Available electronically at http://www.osti.gov/bridge

Available for a processing fee to U.S. Department of Energy
and its contractors, in paper, from:

U.S. Department of Energy
Office of Scientific and Technical Information
P.O. Box 62
Oak Ridge, TN 37831-0062
phone: 865.576.8401
fax: 865.576.5728
email: reports@adonis.osti.gov

Available for sale to the public, in paper, from:

U.S. Department of Commerce
National Technical Information Service
5285 Port Royal Road
Springfield, VA 22161
phone: 800.553.6847
fax: 703.605.6900
email: orders@ntis.fedworld.gov
online ordering: http://www.ntis.gov/ordering.htm

Printed on paper containing at least 50% wastepaper, including 20% postconsumer waste

Foreword

The performance of a wind turbine, as measured by annual energy output, is strongly influenced by the efficiency of its drive train components. Indeed, wind turbine designers must carefully evaluate the choice, combination and control of candidate drive train components in the process of optimizing new machines. Erroneous assumptions can lead to poor design choices. Reliable drive train efficiency data may also be essential in analyzing experimental data. If rotor aerodynamic performance is needed, it can only be deduced from measured electrical power and drive train component efficiencies.

In spite of this seemingly compelling requirement, it is rare that a wind-turbine performance analysis attempts to reflect drive train component efficiencies. Frequently, a single numerical value is used to represent drive train efficiency over the entire power-rpm range. This assumption is particularly egregious for variable-speed turbines with power electronic converters.

The subcontract with Electronic Power Conditioning, Inc., (EPC) had as its primary goal the evaluation of a wound-rotor induction generator with soft-switching power converter. However, the scope of work provided a unique opportunity to obtain high-quality efficiency data for several gearboxes and generators, as well as the power converter. Because of this initiative, NREL is now able to publish these data for use by wind turbine designers and analysts.

Care must be taken not to credit these data with universal applicability. The rated power of the tested components is approximately 300 kW. Extrapolation to larger and smaller sizes should be done cautiously. The power converter that was tested was only a second-generation model of an innovative soft-switching topology. Other configurations will produce different results. Indeed, recent implementations of power converters achieve much higher efficiencies. Notwithstanding these limitations, it is our hope and expectation that the data contained in this report will be useful to our industry partners.

The subcontract that resulted in this report was an arduous effort involving extensive laboratory and field-testing. Special recognition is warranted for industry representatives Claus Weigand of EPC, Tim McCoy and Dayton Griffin of Global Energy Concepts, Inc. (formerly Advanced Wind Turbines, Inc.) At NREL, Brian Gregory, Greg Heine, Scott Larwood, and Kirk Pierce deserve special recognition and thanks.

Paul Migliore

NREL Senior Project Leader

Abstract

In 1993, the National Renewable Energy Laboratory (NREL) awarded Electronic Power Conditioning, Inc., (EPC) a subcontract under which EPC designed, built and tested variable-speed generator systems (VSGS) as retrofits for two different existing fixed-speed turbine designs. The VSGS were tested in the laboratory and in the field. One of the VSGS designs was for the Advanced Wind Turbines, Inc., (AWT) model AWT-26 wind turbine. That design was tested at the National Wind Technology Center (NWTC) test site on an AWT-26 prototype known as "P3." To support this design and testing program, EPC and AWT carried out laboratory tests of drivetrain component efficiencies.

The AWT gearbox tests involved three different models of Flender PZBS-170 (two-stage, planetary) gearboxes. The test results showed that the gearbox power losses resulted mainly from oil churning, depended strongly on oil temperature, increased rapidly with shaft rotation speed, and increased weakly with gearbox load. At a given (low-speed shaft) rotational speed, the power losses were found to be independent of both gearing ratio and rotation direction.

EPC laboratory testing included both the original P3 induction generator at fixed speed, and the doubly-fed generator / power converter VSGS system that EPC designed for variable-speed operation of P3. The fixed-speed induction generator had higher efficiency than the VSGS at all power levels.

In this report, we present the methods used to analyze and apply the measured drivetrain efficiencies and compare the fixed-speed and variable-speed drivetrain efficiencies. We have included a set of hyperbolic curves to provide an accurate and convenient fit to the measured efficiencies.

To develop an illustrative comparison of component and drivetrain efficiencies, we used AWT-26 operational parameters. Because of the improved efficiency at low rotation speeds, the variable-speed gearbox has higher efficiencies than those realized during fixed-speed operation, particularly at low power levels. In contrast, the fixed-speed induction generator has higher efficiencies than the VSGS at all power levels. Evaluation of the total drivetrain shows that the gearbox efficiency gains from variable-speed operation do not offset the additional losses of the VSGS, and as a result, the fixed-speed drivetrain efficiencies are higher than those for the variable-speed drivetrain.

This report was co-edited by Paul Migliore of the NWTC and Dayton Griffin of Global Energy Concepts, L.L.C. (GEC). Dr. Migliore was the NREL Technical Monitor for all of the drivetrain component test activities. As a previous employee of AWT, Mr. Griffin was directly involved in the gearbox testing and also worked collaboratively with EPC to evaluate the potential for variable-speed operation of AWT turbines.

Abbreviations

ANSI	American National Standards Institute
AWT	Advanced Wind Turbines, Inc.
calc'd	calculated
C	degrees Celsius
CCW	counterclockwise
COE	cost of energy
CW	clockwise
DFG	doubly-fed generator
EPC	Electronic Power Conditioning, Inc.
ft	foot, feet
HS	high-speed
KVA	kilovolt-amps
kW	kilowatt
lb	pounds force
LED	light-emitting diode
LS	low-speed
m	meter, meters
meas'd	measured
MW	megawatt
N	Newtons force
NREL	National Renewable Energy Laboratory
NWTC	National Wind Technology Center
P3	AWT-26 prototype turbine located at NWTC
rpm	revolutions per minute
TSR	tip-speed ratio
TSR_{Design}	design tip-speed ratio
USRC	unipolar series-resonant converter
VAC	voltage, alternating current
VSGS	variable-speed generation system

List of Symbols

C_{Pmax}	maximum rotor power coefficient
C_1, C_2	coefficients for hyperbolic curve fits
F	measured force (lb)
$Loss_{Avg}$	average power loss per gearbox (kW)
P_{Grid}	measured grid active power (kW)
P_{HSS}	mechanical power at gearbox high-speed shaft (kW)
$P_{HSS,1}$	high-speed shaft power of first gearbox in test power flow (kW)
P_{in}	input power to component (kW)
P_{Mech}	mechanical power at generator drive shaft (kW)
P_{Rotor}	measured rotor active power of the DFG (kW)
P_{Stator}	measured stator active power of the DFG (kW)
rpm_{DFG}	rotational speed of DFG input shaft (rpm)
T	torque at generator drive shaft (ft lb)
TSR_{Design}	tip-speed ratio at maximum rotor power coefficient
η	component efficiency (%)
η_{DFG}	DFG efficiency (%)
η_{GB}	gearbox efficiency (%)
$\eta_{GB,1}$	efficiency of first gearbox in test power flow (%)
η_{Gen}	efficiency of generator system (%)
η_{USRC}	USRC efficiency (%)
η_{VSGS}	VSGS efficiency (%)
Ω_{HSS}	high-speed shaft rotational speed (rpm)
Ω_{Gen}	generator drive-shaft rotational speed (rpm)
ρ	air density (kg/m^3)

Table of Contents

List of Figures

List of Tables

1. Introduction

1.1 Background

In 1993, the National Renewable Energy Laboratory (NREL) awarded Electronic Power Conditioning, Inc., (EPC) a subcontract under which EPC designed, built and tested variable-speed generator systems (VSGS) as retrofits for two different existing fixed-speed turbine designs (Weigand, Lauw and Marckx, 2000). EPC tested the VSGS design in the laboratory and the field. One of the VSGS designs was for the Advanced Wind Turbines, Inc., (AWT) model AWT-26 wind turbine. This design was tested at the National Wind Technology Center (NWTC) test site on a AWT-26 prototype known as "P3."

To support this design and testing program, EPC and AWT conducted laboratory tests of drivetrain component efficiencies. The AWT tests involved Flender PZBS-170 gearboxes, both for the fixed-speed P3 turbine and the variable-speed retrofit. The EPC testing included the original P3 induction generator in fixed-speed operation, and a doubly-fed generator (DFG)/power converter system designed specifically for use on the P3 turbine.

This report was co-edited by Paul Migliore of the NWTC and Dayton Griffin of Global Energy Concepts, L.L.C., (GEC). Dr. Migliore was the NREL Technical Monitor for all of the drivetrain component test activities. As a previous employee of AWT, Mr. Griffin was directly involved in the gearbox testing and also worked collaboratively with EPC to evaluate the potential for variable-speed operation of AWT turbines.

1.2 Purpose

We intend this report to formally document the conduct and results of the EPC and AWT laboratory testing of drivetrain component efficiencies, and to present the information in a format that will be useful to wind turbine designers and wind energy researchers.

1.3 Scope

In this report, we describe the AWT laboratory testing of two Flender PZBS-170 gearboxes, one used for fixed-speed operation of the P3 turbine, and one geared specifically for the EPC variable-speed retrofit. We also report on the EPC laboratory testing of the P3 induction generator at fixed speed, along with the DFG/power converter VSGS system that EPC designed for variable-speed operation of P3. We summarize the test design, configuration, instrumentation, conduct, and results of these tests. The measured efficiency curves are presented for each component independently. Next, we use the component efficiency curves to compare complete drivetrain efficiencies for the fixed-speed and variable-speed systems, as applied to the operation of the AWT-26 turbine.

1.4 Test Objectives

The overall objectives of the EPC and AWT laboratory testing were to measure the drivetrain component efficiencies for both the original fixed-speed P3 turbine, and for the EPC variable-speed retrofit. Once obtained, these data were used to compare the overall drivetrain efficiencies of the original and modified turbines and to predict the incremental change in the cost of energy (COE) for variable-speed operation. We also used the efficiency data to assess the turbine field test results, inferring rotor power from measurements of the turbine system power performance.

2. Gearbox Laboratory Tests

2.1 Overview

During May and June of 1997, engineers conducted two gearbox efficiency tests at GearWorks, Inc., in Seattle, Washington. Both tests were done on Flender PZBS-170 gearboxes, the model used for the AWT-26 and AWT-27 turbines. The Flender PZBS-170 is a two-stage gearbox with a planetary arrangement of gears in each stage.

The first test was conducted on a PZBS-170 gearbox with a gear ratio of 1:26.07 (designated Mark III), which was manufactured for variable-speed operation of the P3 AWT-26 prototype at the NWTC. To characterize the gearbox efficiencies for the expected operating conditions, the engineers tested the Mark III gearbox under a wide range of rotational speeds, power levels, and temperatures.

The second test was performed on a PZBS-170 with a gear ratio of 1:31.5 gearbox (designated Mark II). The Mark II had been operating at fixed speed on the original P3 turbine. Because the objective of the Mark II test was to quantify the baseline P3 drivetrain efficiencies, the engineers tested the Mark II at a range of load levels, but at only one rotational speed.

For each of the two tests, a secondary gearbox was a part of the test system. For both tests, the secondary gearbox was a PZBS-170 with a gear ratio of 1:28.47 (designated Mark V).

2.2 Gearbox Test Goals and Objectives

The first test was designed to measure the Mark III power losses over a range of rotational speeds, power levels and temperatures. However, because of the experimental setup only the losses from the total system (Mark III and Mark V) could be directly measured, and the testers had to make some assumptions to infer Mark III efficiency from these test results. To increase the confidence in this method, test cases were added to Test #1. The additional test runs were intended to determine:

- If the Mark V efficiencies were measurably different than those measured for the Mark III
- If the gearbox losses were dependent on whether a box is being driven (power supplied *to* the low-speed shaft) or is driving (power supplied *through* the low-speed shaft)
- Whether the losses are dependent on the direction of shaft rotation.

To the extent possible, each item above was resolved in Test #1. The objective of Test #2, then, was then to measure the Mark II losses for a range of power levels, but at the fixed rotational speed that is representative of its field operation on the P3 prototype at the NWTC.

2.3 Test Configuration

The test configuration, instrumentation, and conduct, along with the analysis methods, were nominally the same for both the Mark III and Mark II gearboxes. In the sections that follow, we describe the test configuration and conduct for both tests, and make distinctions between the two tests where necessary.

2.3.1 Test Setup

To run the efficiency tests, two similar PZBS-170 gearboxes were bolted "nose-to-nose" on a test stand, as shown in Figure 2-1. The rectangular cross-section low-speed shafts were coupled with a simple slide-over steel sleeve with Teflon bushings. Testers coupled a dynamometer to each of the gearbox high-speed shafts. As indicated in Figure 2-1, the primary test gearboxes (Mark III and Mark II) were alternately mounted on the north end of the test stand. The secondary test box (Mark V) was mounted at the south end. Table 2-1 documents the test configurations, and Figure 2-2 is a photograph of the PZBS-170 gearboxes on the test stand at GearWorks, Inc.

Table 2-1. Summary of Gearbox Efficiency Test Configurations

Test	Dates	Primary Test Gearbox	Secondary Test Gearbox
Test #1 (variable power level and speed)	04/30/97 through 05/09/97	PZBS-170, Mark III gear ratio: 1:26.07 serial #: D41-612-698-1-1	PZBS-170, Mark V gear ratio: 1:28.47 serial #: D43-412-516-5-5
Test #2 (variable power at fixed speed)	06/11/97 through 06/12/97	PZBS-170, Mark II gear ratio: 1:31.5 serial #: D43-304-550-3-1	same as Test #1

During testing, one dynamometer was used for power input (driving) and the other for power output (driven). Each dynamometer could be used for either power input or power output, and the test apparatus could rotate in either direction. To document the test conditions, the data collectors established the conventions described below. "Forward" power flow indicates that the primary test gearbox has power input to the low-speed shaft, with its high-speed shaft driving the output dynamometer. "Reverse" power flow indicates that power is being input to the high-speed shaft of the primary test gearbox. Shaft rotation directions for each gearbox are always specified as being viewed from the high-speed toward the low-speed shaft (meaning that the viewer is assumed to be facing downwind for normal operation of AWT-26 and AWT-27 turbines).

In general, the dynamometers could be controlled for either rotational speed (rpm) or power level. During testing, the driving (input) unit was controlled for rpm, while the driven dynamometer was controlled for power output. Torque was measured for each dynamometer using a load cell that reacted a lever arm positioned 61 cm (24 inches) from the center of rotation.

The power levels that could be tested were constrained by the test dynamometers, which were limited to a maximum torque of 610 N-m (450 ft lb). At a rotational speed of 32 rpm (low-speed shaft), the test output power was limited to a maximum of about 50 kW, and for speeds of 57 rpm and greater, power levels as high as 100 kW could be achieved. Because the engineers were primarily interested in the lower end of the efficiency curves, the test was not significantly compromised by these limits.

For each gearbox, testers measured the no-load power losses by sliding the low-speed shaft coupler to one side and measuring the torque required to spin each box at varying speeds.

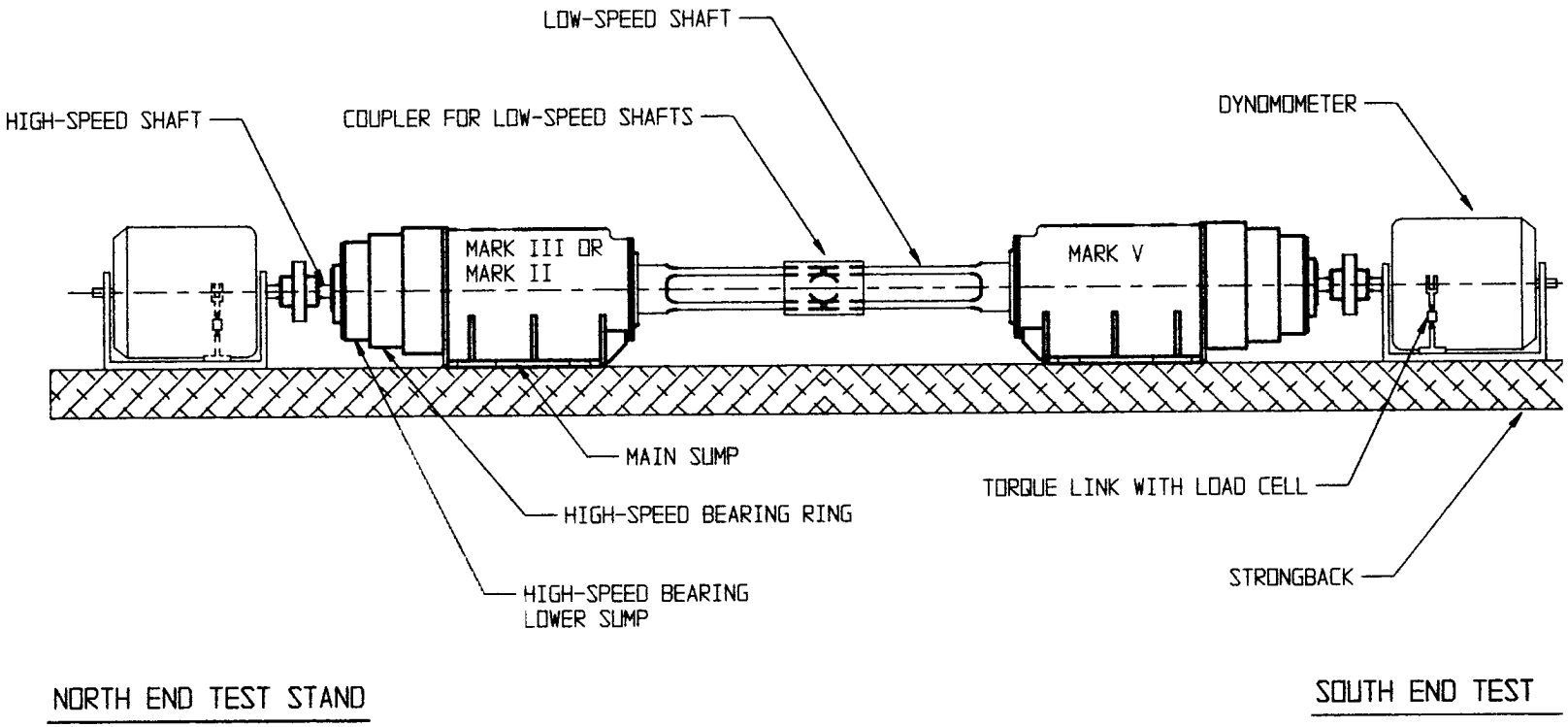

Figure 2-1. Setup for efficiency testing of Flender PZBS-170 gearboxes

Figure 2-2. Flender PZBS-170 gearboxes on the test stand at GearWorks, Inc.

2.3.2 Instrumentation

As indicated above, torque was measured at each dynamometer using load cells with a range of ± 272 kg (600 lb). The load cells were calibrated at the National Standards Testing Laboratory on February 20, 1996. Before each test, the data collectors checked the load cell calibrations by hanging dead weights. During the test, they observed that the load cells experienced a larger-than expected zero-drift resulting from temperature changes. Additionally, significant nonlinearity was observed for the load cells at low force values. Section 2.5.1 covers both issues in more detail.

Each dynamometer was instrumented with a proximity switch to measure shaft rotational speed. Light-emitting diode (LED) screens were mounted on the control boxes of each dynamometer: these screens displayed the output from the load cells and proximity switches in pounds force and rpm. For each test condition, the testers recorded the LED-displayed values by hand on test data sheets. The test precision was determined by the data collectors' ability to mentally time-average the LED-displayed values, and was therefore limited to approximately to ± 0.2 lb and ± 1 rpm.

The test gearboxes were instrumented with American National Standards Institute (ANSI) Type J thermocouples for measuring oil temperature. The thermocouples were inserted into the gearbox interior at several locations. To measure the ambient air temperature, an additional thermocouple was placed external to the gearboxes. The thermocouples were connected to a signal conditioner and a digital readout with a manual switch to determine which channel was displayed. Tables 2-2 and 2-3 document the thermocouple locations, and their assigned channel numbers for each test. Each gearbox was instrumented with a manometer tube to measure oil levels.

Table 2-2. Test #1 Thermocouple Locations and Channel Numbers

	Channel Number	
Location	**Mark III**	**Mark V**
Ambient	1	same
Main sump	5	9
High-speed bearing ring	4	7
High-speed bearing lower sump	3	8

Table 2-3. Test #2 Thermocouple Locations and Channel Numbers

	Channel Number	
Location	**Mark II**	**Mark V**
Ambient	1	same
Main sump	4	10
High-speed bearing ring	2	8
Low-speed bearing ring	3	9
High-speed bearing lower sump	not used	7

2.4 Test Conduct

2.4.1 Test Matrices

Table 2-4 shows the nominal test matrix for Test #1. Not all of the possible combinations indicated by the table were tested. As the test progressed, the testers reduced and evaluated the data to determine the best use of available test time and budget. Each test run was logged on a separate data sheet that indicates the test condition, date, and measurements recorded. The test matrix for Test #2 was a subset of Table 2-4, with all testing performed with hot oil temperatures and a fixed rotational speed of 57.8 rpm (low-speed shaft).

Table 2-4. Nominal Test Matrix for Gearbox Efficiency Test #1

Rotational Speed (low-speed shaft)	Oil Temp.	Load Condition	Power Flow	Rotation
32-62 rpm, in 5-rpm increments	cold	no-load	reverse	both directions
32-62 rpm, in 5-rpm increments	hot	no-load	reverse	both directions
32-62 rpm, in 5-rpm increments	hot	5-100 kW (output), or 5 kW to maximum	forward / reverse	both directions

Note that reverse is the only power flow direction indicated for the no-load tests. With the low-speed shafts decoupled, the only way the dynamometers could drive the gearboxes was in reverse relative to normal operation. Also note that for testing under load, the designation of forward or reverse is only given for the primary test box (Mark III or Mark II). With the primary gearbox driven forward, the secondary gearbox (Mark V) is necessarily being driven in reverse.

Tables 2-5 and 2-6 show examples of detailed test matrices used for specific runs. Table 2-5 is for varying rpm at a no-load condition; Table 2-6 is for varying load at a constant rpm.

Table 2-5. No-Load Test Matrix for Mark III Gearbox (Test #1)

LS Shaft (rpm)	Oil Temp.	HS Shaft (rpm)	Force (lb)	Input Power (kW)	Output Power (kW)
32	hot	834	required	calculated	0
37	hot	965	required	calculated	0
42	hot	1,095	required	calculated	0
47	hot	1,225	required	calculated	0
52	hot	1,356	required	calculated	0
57	hot	1,486	required	calculated	0
62	hot	1,616	required	calculated	0
32	hot	834	required	calculated	0

Table 2-6. Test Matrix for Loaded Mark III Gearbox at 62 rpm (Test #1)

		AWT Mark V, 1:28.47				EPC Mark III, 1:26.07			
LS Shaft (rpm)	Oil Temp.	HS Shaft (rpm)	Force (lb)	Input (kW)	Output (kW)	HS Shaft	Force (lbs)	Input (kW)	Output (kW)
62	hot	1,765	meas'd	calc'd	N/A	1,616	10.9	N/A	5.0
62	hot	1,765	meas'd	calc'd	N/A	1,616	21.8	N/A	10.0
62	hot	1,765	meas'd	calc'd	N/A	1,616	32.7	N/A	15.0
62	hot	1,765	meas'd	calc'd	N/A	1,616	43.7	N/A	20.0
62	hot	1,765	meas'd	calc'd	N/A	1,616	65.5	N/A	30.0
62	hot	1,765	meas'd	calc'd	N/A	1,616	87.3	N/A	40.0
62	hot	1,765	meas'd	calc'd	N/A	1,616	109.2	N/A	50.0
62	hot	1,765	meas'd	calc'd	N/A	1,616	163.2	N/A	75.0
62	hot	1,765	meas'd	meas'd	N/A	1,616	218.3	N/A	100.0
62	hot	1,765	meas'd	calc'd	N/A	1,616	10.9	N/A	5.0

N/A: not applicable

The designation hot means that the gearbox oil was at its nominal operating equilibrium temperature for the test lab conditions. Cold means that the oil temperature was initially at ambient room temperature. Temperature management was a challenging aspect of the test conduct, as the operating temperatures are highly dependent on rotational speed. For all runs, the testers recorded the gearbox oil temperatures on the test data sheets.

Each gearbox was thoroughly flushed and drained before testing, then filled to the desired level with fresh lubricant. In previous work, AWT measured the dependence of both efficiency and temperature on oil level for PZBS-170 gearboxes (February 1996). For the work described here, all three test boxes were filled with Tribol 800/220 type synthetic oil, nominally 15 gallons each. For Test #1, the objective was to have both boxes filled to the same level. The testers used manometer tubes to measure the oil level. The Mark III and Mark V boxes were both filled to approximately 7 cm (2.75 in.) below the shaft centerline. For Test #2, the Mark II gearbox was tested with the oil level unchanged from its recent operating condition at the NWTC.

2.4.2 Data Acquisition and Reduction

For each test run, the data collectors recorded the data by hand on test data sheets. Figure 2-3 shows an example of a data sheet which was completed on May 8, 1997 during Test #1. The data sheets contain the test run number, date, test configuration, and time of each observation. The test run recorded in Figure 2-3 (Run #24 from Test #1), corresponds to the test matrix shown in Table 2-6, with the Mark III high-speed shaft at a nominal speed of 1,616 rpm and the actuator force varied through the predetermined schedule. At each test point, the testers recorded the measured shaft speeds and torque-arm forces, along with ambient and gearbox temperatures.

The test data sheets also contain data reduction columns for input and output power, average power loss, and average efficiency. During the test, these columns were used to spot-check the test results.

Input and output power was calculated at the gearbox high-speed shafts as the product of torque times rotational speed:

$$P_{HSS} = 2.834 \cdot 10^{-4} \cdot \Omega_{HSS} \cdot F \qquad \text{(Eqn. 2-1)}$$

where

P_{HSS} ≡ mechanical power at high-speed shaft (kW)

Ω_{HSS} ≡ high-speed shaft rotational speed (rpm)

F ≡ force at reacting lever arm (lb).

The total power loss was calculated from the difference between the input and output power as measured at the high-speed shafts. The average power loss for each box was obtained by assuming that the power loss was divided equally between the two boxes. The efficiency of the first gearbox in the power flow was derived by:

$$\eta_{GB,1} = 100 \cdot \left(1 - \left(\frac{Loss_{Avg}}{P_{HSS,1}} \right) \right) \qquad \text{(Eqn. 2-2)}$$

where

$\eta_{GB,1}$ ≡ efficiency of the first gearbox in power flow direction of test (%)

$Loss_{Avg}$ ≡ average power loss per gearbox (kW)

$P_{HSS,1}$ ≡ high-speed shaft power of first gearbox in power flow (kW)

In principle, the efficiency for the second gearbox in the power flow direction could be calculated in an analogous manner, where the power input to the second gearbox is calculated as the difference between $P_{HSS,1}$ and $Loss_{Avg}$. However, we calculated all the data presented in this report using the method of Equation 2-2.

Following each day of testing, the hand-logged data were typed into a spreadsheet, where Equations 2-1 and 2-2 were used to calculate input power, input power, and average power loss and efficiency values. Figure 2-4 shows the data reduction spreadsheet used for Test #1 (Run #24).

Test #2 used similar data logs and data reduction spreadsheets, with the exception of adding a column for “adjusted” force measurements, where the adjustment was made for the observed nonlinear behavior of the load cells near zero force.

Run # 24 Description 62 Rpm (LSS)

Date 5-8-97 MARK III DRIVEN (Repeat of Run #3)

AWT Mark V, 1:28.47, Ser. D43-412-

EPC Mark III, 1:26.07, Ser. D41-612-

Time (hours)	Ambient Temp (deg F)	AWT Mark V, 1:28.47 INPUT THC 7 (deg F)	THC 8 (deg F)	THC 9 (deg F)	HS Shaft (rpm)	Force (lbs)	HS Power (kW)	EPC Mark III, 1:26.07 OUTPUT THC 3 (deg F)	THC 4 (deg F)	THC 5 (deg F)	HS Shaft (rpm)	Force (lbs)	HS Power (kW)	Avg. Pwr Loss (kW)
14:30	75	203	203	153	1765	26.1		196	196	151	1617	11.1		
14:35	75	202	202	153	1765	35.9		197	197	151	1616	21.9		
14:36	75	202	202	153	1764	45.9		197	197	151	1617	32.7		
14:38	75				1764	56.1					1616	43.7		
14:39					1764	76.4					1615	65.6		
14:42					1765	95.8					1617	87.2		
14:42	74	203	203	153	1765	116.9		197	197	152	1617	109.2		
14:45					1766	167.1					1616	153.5		
14:48	74	203	203	154	1766	201.0		198	197	152	1617	199.6		
14:50	74	203	203	154	1765	26.2		198	197	152	1615	11.3		

Oil Type: Tribol 800/220 (both boxes)

Oil Level: 15 gallons (nominal both boxes)

" 13.0 INCHES ABOVE FOOT (MEASURED, BOTH BOXES)

THC 3 & 7: HS BEARING LOWER SUMP

THC 4 & 8: HS RING

THC 5 & 9: MAIN SUMP

Figure 2-3. Original data sheet for gearbox Test #1 (Run #24 shown)

	B	C	D	E	F	G	H	I	J	K	L	M	N	O	P	Q
1						GearWorks Efficiency Test of Flender PZBS 170 Gearboxes										
2																
3	Run #	24 of 35				Description	62 rpm (LSS)						AWT Mark V, 1:28.47, Ser. # D43-412-516-5-5			
4	Date	05-08-97					Mark III Driven (Repeat of Run #3)						EPC Mark III, 1:26.07, Ser. # D41-612-698-1-1			
5																
6		Ambient	AWT Mark V, 1:28.47					input	EPC Mark III, 1:26.07					output	Avg. Pwr.	Avg.
7	Time	Temp	THC 7	THC 8	THC 9	HS Shaft	Force	HS Power	THC 3	THC 4	THC 5	HS Shaft	Force	HS Power	Loss	Effic.
8	(hours)	(deg F)	(deg F)	(deg F)	(deg F)	(rpm)	(lbs)	(kW)	(deg F)	(deg F)	(deg F)	(rpm)	(lbs)	(kW)	(kW)	(%)
9	14:30	75	203	203	153	1765	26.1	13.06	196	196	151	1617	11.1	5.09	3.98	69.5
10	14:35	75	202	202	153	1765	35.9	17.96	197	197	151	1616	21.9	10.03	3.96	77.9
11	14:36	75	202	202	153	1764	45.9	22.95	197	197	151	1617	32.7	14.99	3.98	82.7
12	14:38	75				1764	56.1	28.05				1616	43.7	20.01	4.02	85.7
13	14:39					1764	76.4	38.19				1615	65.6	30.02	4.08	89.3
14	14:42					1765	95.8	47.92				1617	87.2	39.96	3.98	91.7
15	14:42	74	203	203	153	1765	116.4	58.22	197	197	152	1617	109.2	50.04	4.09	93.0
16	14:45					1766	167.1	83.63				1616	163.5	74.88	4.38	94.8
17	14:48	74	203	203	154	1766	201.0	100.60	198	197	152	1617	199.6	91.47	4.56	95.5
18	14:50	74	203	203	154	1765	26.2	13.11	198	197	152	1615	11.3	5.17	3.97	69.7
19																
20																
21	Oil Type:	Tribol 800/220 (both boxes)						THC 3 & 5	High-speed bearing lower sump				All directions specified as viewed			
22	Oil Level:	15 gallons (nominal both boxes)						THC 4 & 6	High-speed bearing ring				facing downwind.			
23		13.0 inches above foot (measured, both boxes)						THC 5 & 9	Main sump							

Figure 2-4. Data reduction spreadsheet for gearbox Test #1 (Run #24 shown)

2.5 Test Results

2.5.1 Data Reliability and Test Troubleshooting

After the first day of testing during Test #1 (May 1, 1997), the data collectors observed some unexpected trends. In particular, the results showed a higher-than-expected dependency on power flow direction. This unexpected behavior motivated a second day of testing for Test #1 to further investigate dependencies on power flow direction, and to confirm the data from May 1. Additionally, a gearbox specialist was consulted about physical loss mechanisms and expected dependencies for the Flender PZB model gearboxes (McVittie, 1997). Table 2-7 summarizes this consultation. Although the discussion was primarily focused on the Flender PZBS-170 (two-stage, planetary) gearboxes, similar loss mechanisms and dependencies would be expected for most other gearbox designs.

Table 2-7. Loss Mechanisms and Expected Dependencies for Flender PZBS Gearboxes

Loss Mechanisms	Expected Dependencies (first-order)
Gear mesh churning and bearing churning (oil)	Highly dependent on oil temperature Dependent on rotational speed, correlated with low-speed shaft Independent of load and rotation direction
Seal friction losses	Independent of load, rotational speed and direction
Bearing losses	Approximately linear with load Independent of rotational speed and direction
Gear mesh friction	Approximately linear with load May show slight dependence on direction depending on gear-tooth cutting and wear

A second day of testing for Test #1 was conducted on May 8, 1997. Because of the anomalous trends observed from the May 1 data, testers took additional care in checking the load cell zero and confirming the calibrations by hanging weights. During this effort, they observed that:

- The load cells showed a larger-than-expected zero drift, correlated with ambient temperature.
- The load cells calibration was nonlinear near zero load, with the most pronounced nonlinear behavior in the range between ± 25 lb.

On May 9, 1997, the nonlinear calibration near zero was carefully measured for each load cell. Figure 2-5 shows the result of these measurements. Additionally, the no-load test cases were re-run for each gearbox (Mark III and Mark V), with and without a 65-lb preloading of the load cells. Once the nonlinear calibration had been established, the testers corrected the no-load data from May 8 and compared those data with the May 9 test runs. After these corrections were made, the test data from May 8 were consistent with the expected trends described in Table 2-7. Unfortunately, the data from May 1 could not be corrected with confidence, because of uncertainties in the drift of the load-cell zeros. Most of the Test #1 data from May 1 (Runs #3-#17) were, therefore, not used in the following analyses. Runs #1 and #2 from Test #1 are shown to illustrate the effect of temperature on no-load gearbox losses. However, these data may be slightly erroneous because of the effects noted above.

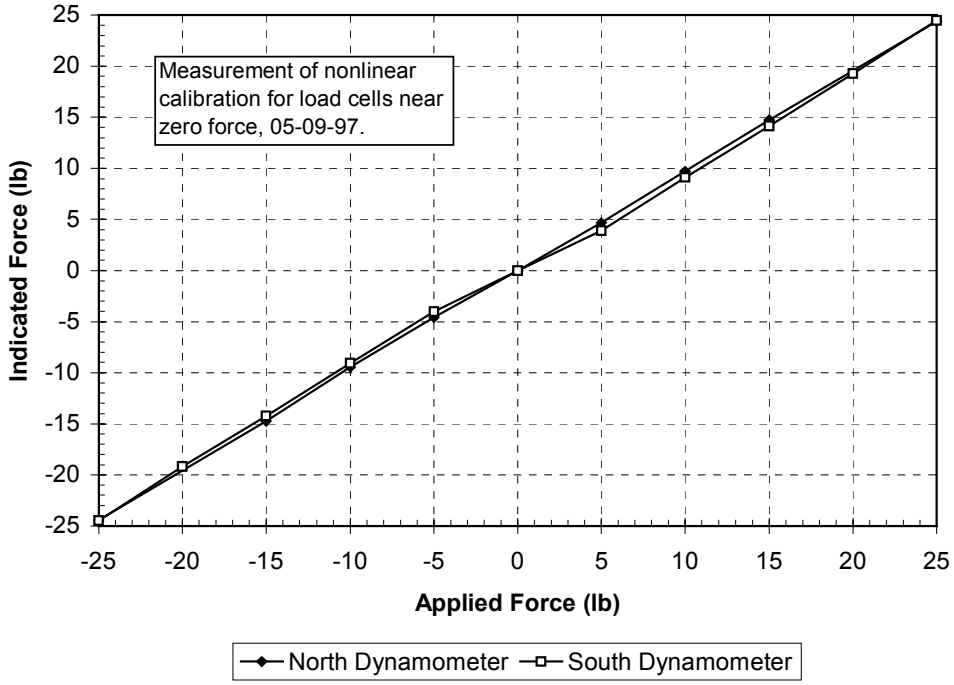

Figure 2-5. Nonlinear calibration of load cells near zero force

A nonlinear calibration, similar to that shown in Figure 2-5, was measured on June 11, 1997, and used to adjust force measurements near zero for Test #2. In addition, the testers took care during Test #2 to maintain the load cell zero and confirm the calibrations. Once the data had been corrected for the nonlinear calibrations near zero force, the test results were entirely consistent with the expected trends listed in Table 2-7.

As discussed above, the testers took care to identify and address issues surrounding the reliability of the measurement equipment throughout the conduct of the gearbox tests. Selecting the highest confidence data sets for reporting required the AWT engineers to apply their judgment. Table 2-8 documents the test runs and conditions that were chosen as the most reliable measurements, and the figures and analyses that follow offer further detail on these test cases. Except where noted, all test cases in Table 2-8 are for the hot operating condition. Most of the no-load data cases reported were measured using a dead-weight preload (bias) in the load cells. The engineers believe this to be the highest confidence measurement method, and for runs that used this approach, the need to apply the nonlinear calibration at near-zero-force-values was eliminated.

Table 2-8. Summary of Highest Confidence Data Sets from Gearbox Testing

Test #	Date	Run #	LS Shaft (rpm)	Test Condition
1	04/30/97	1	varying	Mark III, no-load, CW, cold temperature
1	05/08/97	24	62	Mark III, varying load, forward power flow
1	05/08/97	27	57	Mark III, varying load, reverse power flow
1	05/08/97	29	47	Mark III, varying load, reverse power flow
1	05/08/97	31	37	Mark III, varying load, reverse power flow
1	05/08/97	33	32	Mark III, varying load, forward power flow
1	05/08/97	34	42	Mark III, varying load, forward power flow
1	05/08/97	35	52	Mark III, varying load, forward power flow
1	05/10/97	40	varying	Mark III, no-load, CW, 289 N (65 lb) bias on load cell
1	05/10/97	41	varying	Mark III, no-load, CCW, 289 N (65 lb) bias on load cell
1	05/10/97	42	varying	Mark V, no-load, CCW, 289 N (65 lb) bias on load cell
1	05/10/97	43	varying	Mark III, no-load, CW, 289 N (65 lb) bias on load cell
2	06/12/97	3	57.8	Mark III, no-load, both rotation directions, 334 N (75 lb) bias on load cell
2	06/12/97	5	57.8	Mark II, varying load, forward power flow
2	06/12/97	6	57.8	Mark II, varying load, reverse power flow
2	06/12/97	7	57.8	Mark II, varying load, forward power flow (repeat of Run #7)

2.5.2 Measured Gearbox Efficiencies

In the material that follows, we present the gearbox losses and efficiencies for the two gearbox tests as average values, where the loss in each box is assumed to be one-half of the total system loss. The actual losses will vary in the two gearboxes, with the largest loss in the first driven unit and a slightly smaller loss in the second. However, Heine's work (June 1998a) demonstrated that this differential is negligible, and that simple averaging of losses is a highly accurate method.

The level of care taken in maintaining load-cell calibrations, and hence the data quality, was generally increased throughout the gearbox testing program. The testers completed the no-load measurements of Test #1 and the complete matrix of Test #2 under highly monitored conditions. As described in the following paragraphs, these data were used to establish sensitivities of power losses to power flow direction and shaft rotation direction, which were in turn used to interpret the remaining test data.

Figure 2-6 shows the no-load power losses measured during Test #1 for the Mark III and Mark V gearboxes, with each operated in clockwise and counterclockwise directions. For all cases shown, the load cells were preloaded with 289 N (65 lb) bias before testing. The data for all cases are in close agreement, differing by no more than 0.4 kW at any given rotational speed. The no-load power losses increase steadily with shaft rotational speed.

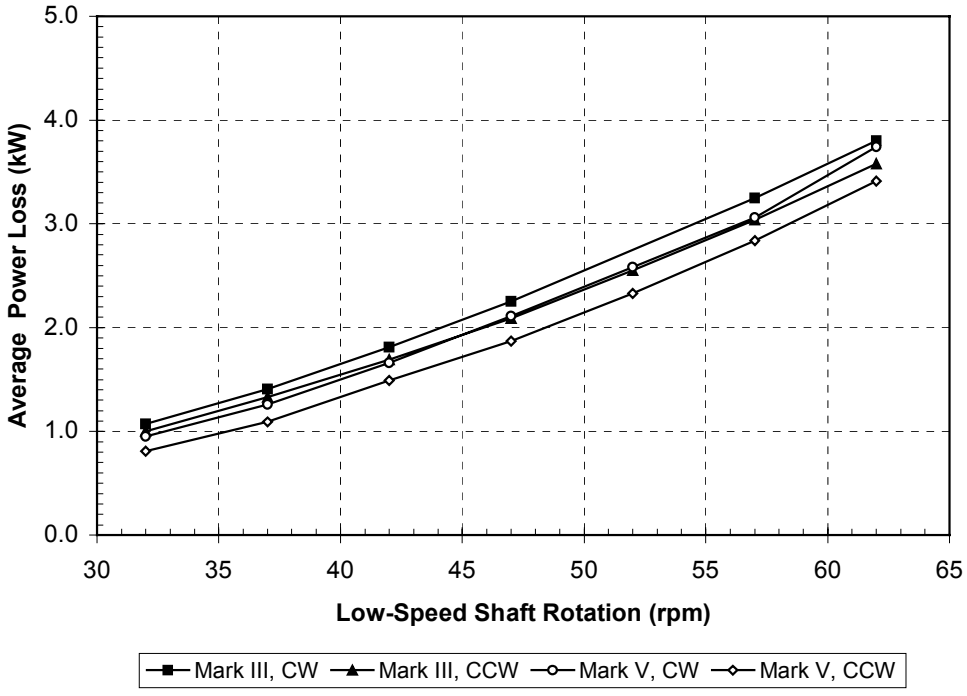

Figure 2-6. No-load power losses from Test #1

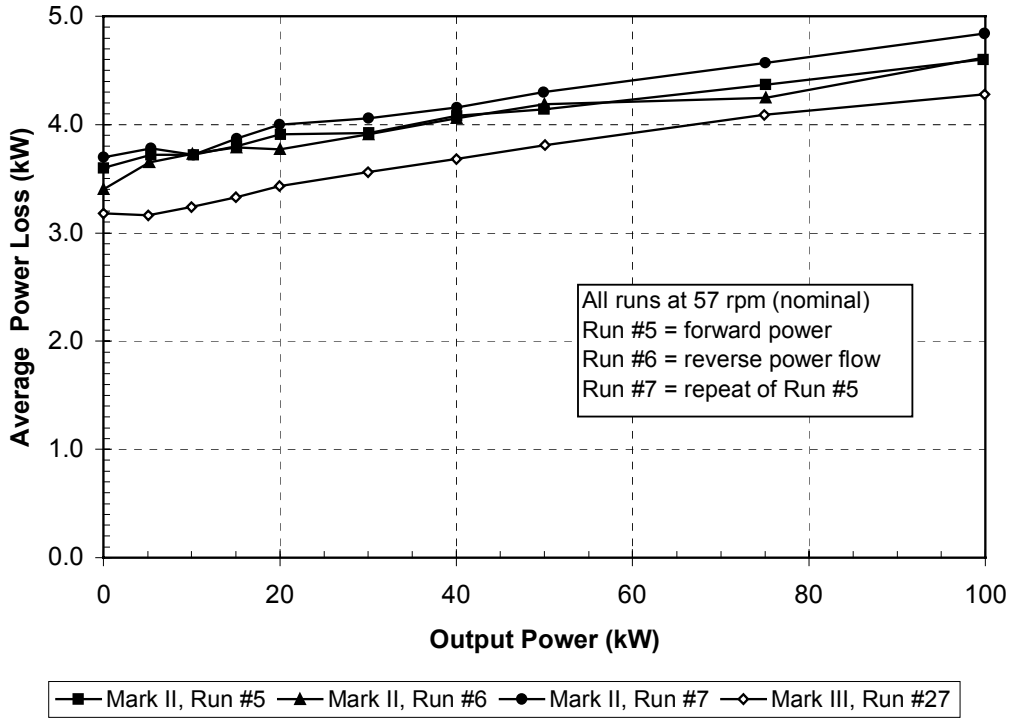

Figure 2-7. Measured power losses at 57 rpm (nominal)

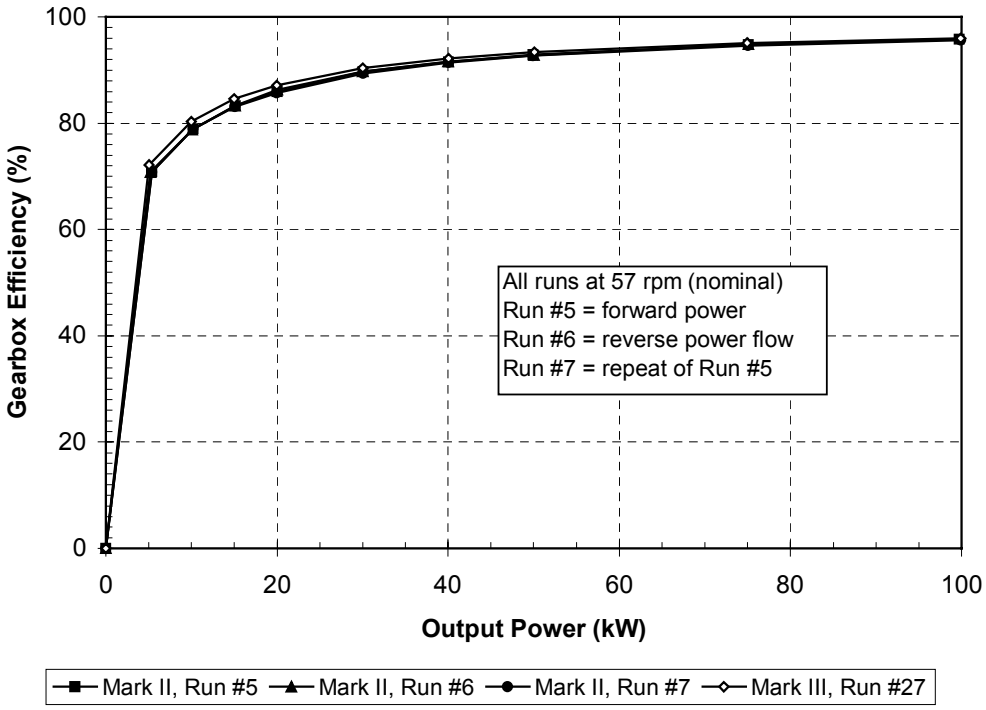

Figure 2-8. Measured efficiencies at 57 rpm (nominal)

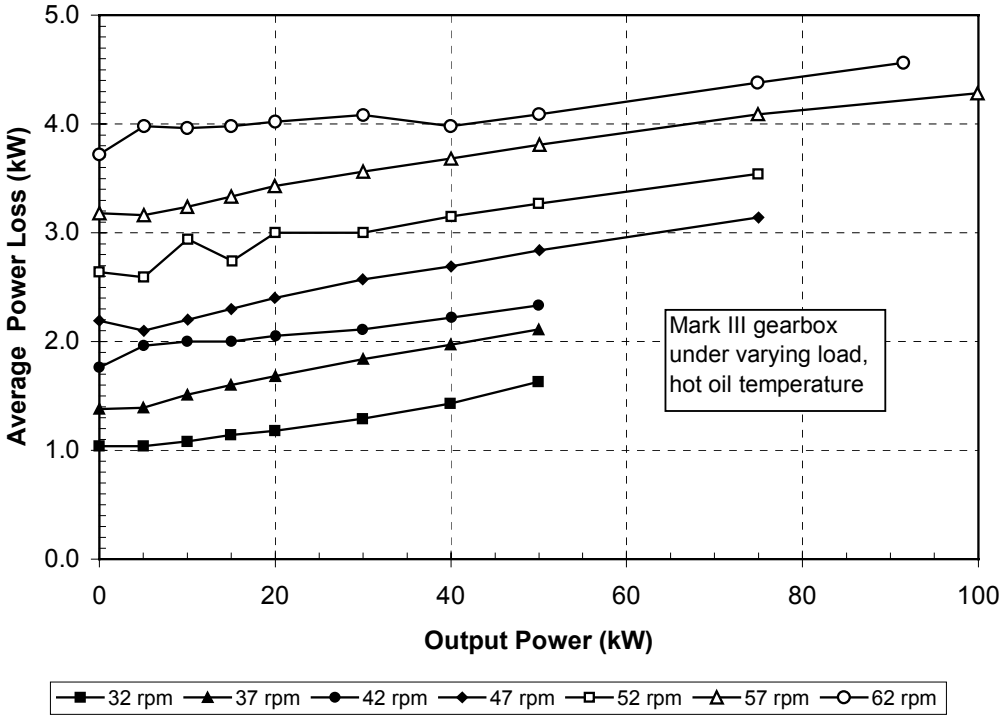

Figure 2-9. Measured power losses for Mark III gearbox

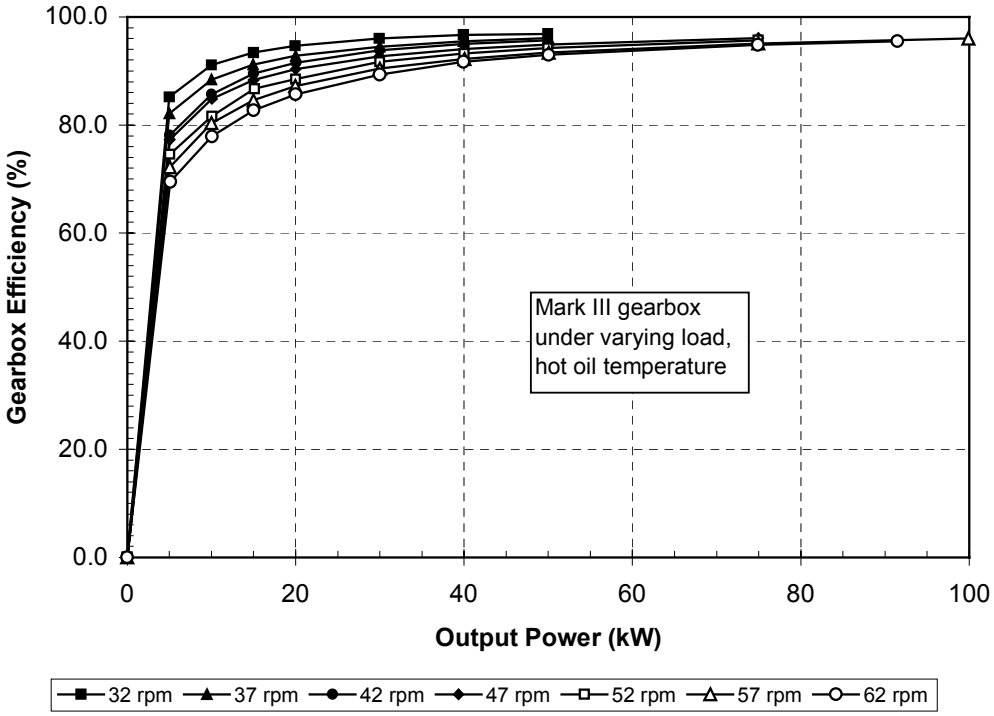

Figure 2-10. Measured efficiencies for Mark III gearbox

Table 2-9. Measured Power Losses and Efficiencies for Mark III Gearbox

	62-rpm Forward Mark III Driven, CW (Run #24)		57-rpm Reverse Mark V Driven, CCW (Run #27)		52-rpm Forward Mark III Driven, CW (Run #35)		47-rpm Reverse Mark V Driven, CCW (Run #29)		42-rpm Forward Mark III Driven, CW (Run #34)		37-rpm Reverse Mark V Driven, CCW (Run #31)		32-rpm Forward Mark III Driven, CW (Run #33)	
Output HS Power (kW)	Avg. Pwr. Loss (kW)	$\eta_{GB,1}$ (%)	Avg. Pwr. Loss (kW)	$\eta_{GB,1}$ (%)	Avg. Pwr. Loss (kW)	$\eta_{GB,1}$ (%)	Avg. Pwr. Loss (kW)	$\eta_{GB,1}$ (%)	Avg. Pwr. Loss (kW)	$\eta_{GB,1}$ (%)	Avg. Pwr. Loss (kW)	$\eta_{GB,1}$ (%)	Avg. Pwr. Loss (kW)	$\eta_{GB,1}$ (%)
0.00	3.72	0.0												
5.09	3.98	69.5												
10.03	3.96	77.9												
14.99	3.98	82.7												
20.01	4.02	85.7												
30.02	4.08	89.3												
39.96	3.98	91.7												
50.04	4.09	93.0												
74.88	4.38	94.8												
91.47	4.56	95.5												
0.00			3.18	0.0										
5.06			3.16	72.2										
9.99			3.24	80.3										
14.99			3.33	84.6										
19.96			3.43	87.2										
30.01			3.56	90.4										
40.04			3.68	92.2										
50.07			3.81	93.4										
74.93			4.09	95.1										
99.90			4.28	96.0										
0.00					2.64	0.0								
5.04					2.59	74.6								
10.08					2.94	81.6								
15.11					2.74	86.7								
20.02					3.00	88.5								
30.01					3.00	91.7								
40.00					3.15	93.2								
49.96					3.27	94.2								
74.94					3.54	95.7								
0.00							2.19	0.0						
5.04							2.10	77.3						
10.05							2.20	84.8						
15.02							2.30	88.3						
19.98							2.40	90.3						
29.96							2.57	92.7						
40.03							2.69	94.1						
50.09							2.84	94.9						
74.97							3.14	96.1						
0.00									1.76	0.0				
5.03									1.96	78.1				
9.99									2.00	85.7				
15.02									2.00	89.5				
20.05									2.05	91.5				
29.98									2.11	93.8				
40.06									2.22	95.0				
49.96									2.33	95.7				
0.00											1.38	0.0		
4.98											1.39	82.1		
9.98											1.51	88.4		
14.97											1.60	91.2		
20.01											1.68	92.8		
29.99											1.84	94.5		
39.96											1.97	95.5		
49.99											2.11	96.1		
0.00													1.04	0.0
4.99													1.04	85.2
10.00													1.08	91.1
14.98													1.14	93.4
19.97													1.18	94.7
29.95													1.29	96.0
39.92													1.43	96.7
49.94													1.63	96.9

Figure 2-11 shows the effect of temperature on the no-load gearbox losses. The increase in churning-losses are substantial for the cold-oil condition, ranging from 2 kW to 4 kW higher than those seen at hot oil temperatures. The data for cold oil operation were taken early in Test #1, and the nonlinear calibration of May 9, 1997, was used to post-correct for the load cell behavior near zero force. As a result, we consider the cold no-load data to be of slightly lower confidence than the remaining data presented. However, the magnitude and trends of temperature effect shown in Figure 2-11 are consistent with the results of AWT (1996), and we believe they accurately characterize the temperature effect on the oil-churning losses.

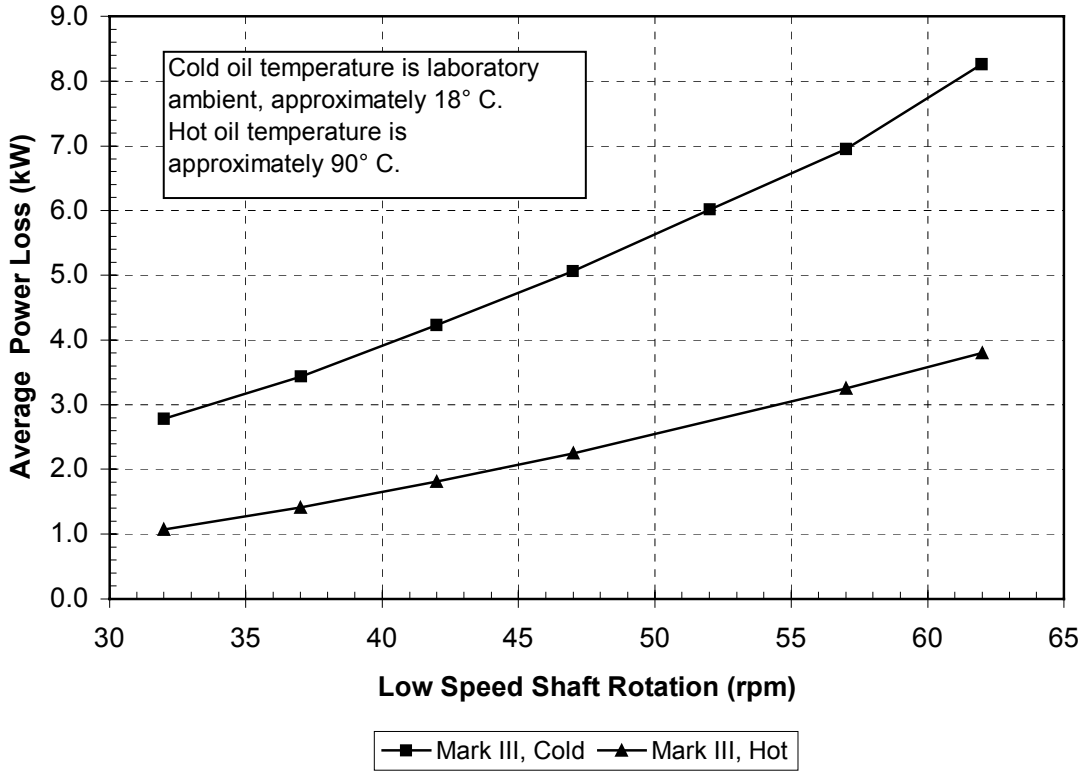

Figure 2-11. Effect of oil temperature on Mark III no-load power losses

3. Generator Laboratory Tests

3.1 Overview

Two generator efficiency tests were conducted at the EPC facilities in Corvallis, Oregon. On June 25, 1997, the VSGS system that EPC designed for retrofit to the AWT-26 turbine (P3) was tested at a schedule of rotational speeds and power levels. The VSGS consisted of a DFG and a unipolar series-resonant converter (USRC).

On March 4, 1998, engineers tested the original induction generator from the P3 turbine at fixed speed.

3.2 Generator Test Goals and Objectives

The objective of the first EPC laboratory test was to measure the efficiency of the VSGS that EPC designed for the variable-speed retrofit of the P3 turbine. The second test was to measure the efficiency of the original induction generator, which was used for fixed-speed operation of P3.

The testers then used these data to compare the overall drivetrain efficiencies of the original and modified turbines and to predict the incremental change in COE for variable-speed operation of the AWT-26. The efficiency data were also used to assess the turbine field test results, where rotor power was inferred from measurements of the turbine system power performance.

3.3 Test Configuration

The testing of the fixed-speed induction generator (Test #2) was a simplified version of the VSGS test, with essentially the same configuration, instrumentation, conduct, and analysis methods. In the sections that follow, we describe the test configuration and conduct for the VSGS test, noting any deviations or exceptions for the fixed-speed tests as appropriate.

3.3.1 Test Setup

The generator efficiency tests were conducted at EPC's variable-speed generation test facility, which is capable of simulating wind turbine operation up to 2,400 rpm (gearbox high-speed shaft), and with up to 375 kW of mechanical power input (Weigand, Lauw and Marckx, 2000). The mechanical output of the wind turbine is simulated by a variable-speed drive operating an induction motor. The variable-speed drive operates on the principle of field-oriented control and can control either the motor torque or the motor rpm. Figure 3-1 shows a block diagram of the test setup, and Figure 3-2 is a photograph of a generator installed in the test facility. The VSGS test equipment is connected to a 750-kVA, 480-VAC utility transformer with an approximate short-circuit impedance of 2.3%. Table 3-1 documents the test articles for each test.

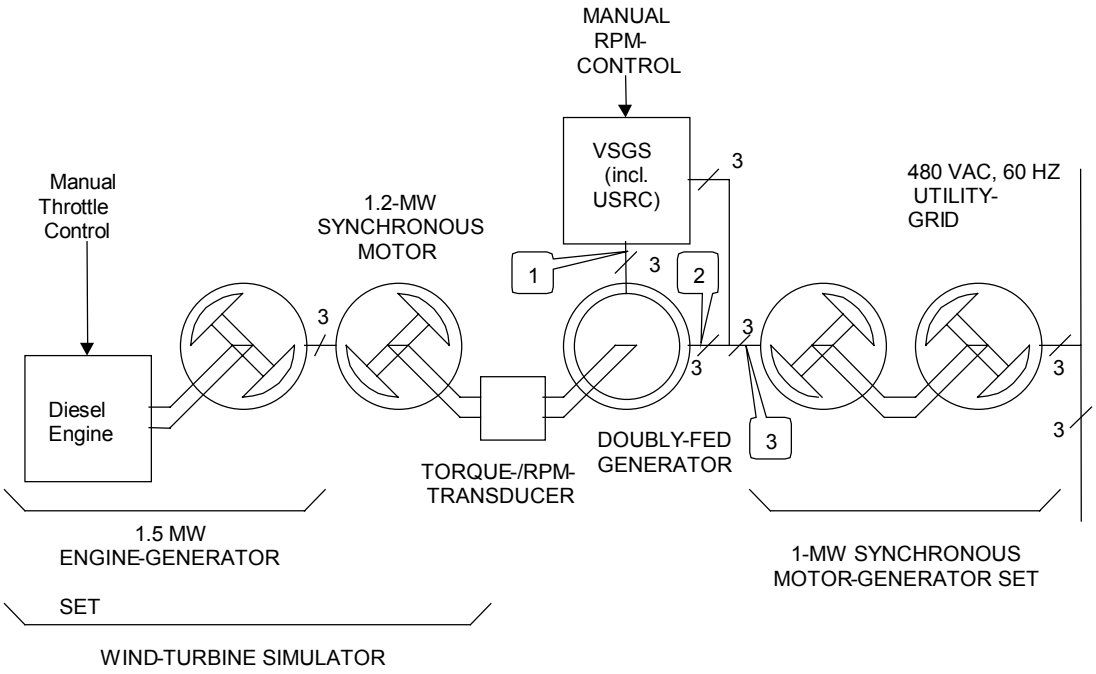

Figure 3-1. Block diagram of 373-kW VSGS wind turbine simulator setup

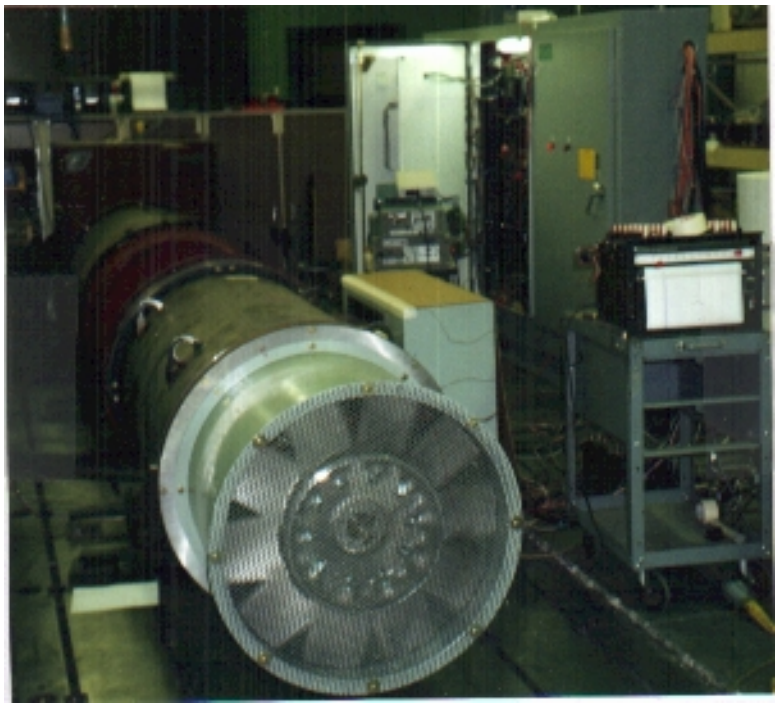

Figure 3-2. EPC's 373-kW VSGS test setup

Table 3-1. Summary of Generator Efficiency Test Configurations

Test	Dates	Test Articles
Test #1 (variable power level and speed)	06/25/97	VSGS consisting of: 1. DFG, Reuland Electric, Model #24031, Serial #CN94-H0259A-1 2. USRC, EPC Inc.
Test #2 variable power at fixed speed)	03/4/98	Induction generator, U.S Electrical Motors, 275 kW, I.D. #B73126/W09W1870980R-2

3.3.2 Instrumentation

Figure 3-1 shows the primary test instruments schematically. Input torque and shaft speed were measured using a Himmelstein MCRT 2807T torque transducer. Power measurements were made at the DFG rotor, DFG stator, and point of common coupling with the utility grid (labeled as points #1, #2 and #3 in Figure 3-1). At each of these three points, Voltech power analyzers (PM3000 series) were used to measure voltage, active power, and reactive power. The torque transducer and power analyzers were connected to a PC-based data acquisition system utilizing LABVIEW® software.

3.4 Test Conduct

3.4.1 Test Matrices

Table 3-2 shows the nominal test matrices for the EPC generator efficiency tests. For Test #1, the schedule of shaft speeds corresponds to low-speed shaft speeds of 32 rpm to 62 rpm, in 5-rpm increments, for the gearing ratio of the variable-speed retrofit of P3. For Test #2, the shaft speed corresponds to the fixed-speed operation of P3, including an adjustment for the expected slip of the induction generator. The as-run test matrices can be seen in Tables 3-3 and 3-4, which give the generator efficiency test results in a tabular format.

Table 3-2. Nominal Test Matrices for EPC Generator Efficiency Tests

Test	Shaft Speed (rpm)	Input Mechanical Power (kW)
#1	834 to 1,616, increments of 130	Schedule of input power at each rpm
#2	1,800 to 1,818, with schedule of speeds to approximate 1% generator slip at rated power	15, 20, 30, 40, 50, 75, 100, 125, 150, 175, 200, 225, 250, 275, 300

3.4.2 Data Acquisition and Reduction

For each test point, engineers used the PC controller to set the variable-speed drive to the desired shaft speed and torque level. The LABVIEW® data acquisition software recorded the torque, speed, and power data. Mechanical power input was calculated from:

$$P_{Mech} = 1.420 \cdot 10^{-4} \cdot \Omega_{Gen} \cdot T \qquad \text{(Eqn. 3-1)}$$

where

P_{Mech} ≡ mechanical power at generator drive shaft (kW)

Ω_{Gen} ≡ generator drive shaft rotational speed (rpm)

T ≡ torque at generator drive shaft (ft lb).

For both the VSGS and fixed-speed induction generator, the electrical system efficiency was calculated from:

$$\eta_{Elect.Sys.} = 100 \cdot \left(\frac{P_{Grid}}{P_{Mech}} \right) \qquad \text{(Eqn. 3-2)}$$

where

$\eta_{Elect.\ Sys.}$ ≡ the electrical system efficiency for either the VSGS or the induction generator (%)

P_{Grid} ≡ measured grid active power (kW)

For the VSGS, the component efficiencies were calculated from P_{Mech} and the three electrical power measurements by:

$$\eta_{USRC} = 100 \cdot \frac{-P_{Rotor}}{(P_{Stator} - P_{Grid})} \quad \text{if } rpm_{DFG} \le 1200 \text{ rpm, and} \qquad \text{(Eqn. 3-3a)}$$

$$\eta_{USRC} = 100 \cdot \frac{(P_{Gridr} - P_{Stator})}{P_{rotor}} \quad \text{if } rpm_{DFG} > 1200 \text{ rpm} \qquad \text{(Eqn. 3-3b)}$$

where

η_{USRC} ≡ USRC efficiency (%)

P_{Rotor} ≡ measured active power at the DFG rotor (kW)

P_{Stator} ≡ measured active power at the DFG stator (kW)

rpm_{DFG} ≡ rotational speed of DFG input shaft (rpm)

$$\eta_{DFG} = 100 \cdot \frac{P_{Stator}}{(P_{Mech} - P_{Rotor})} \quad \text{if } rpm_{DFG} \le 1200 \text{ rpm, and} \qquad \text{(Eqn. 3-4a)}$$

$$\eta_{DFG} = 100 \cdot \frac{(P_{Stator} + P_{Rotor})}{P_{Mech}} \quad \text{if } rpm_{DFG} > 1200 \text{ rpm} \qquad \text{(Eqn. 3-4b)}$$

where

η_{DFG} ≡ DFG efficiency (%)

3.5 Test Results

3.5.1 Variable-Speed Generator System

Figure 3-3 presents the measured VSGS efficiencies graphically. For ease of comparison with the gearbox data, Figure 3-3 shows shaft speeds as equivalent low-speed shaft speeds for the variable-speed operation of P3. Unlike in the gearbox efficiency curves, we can see no clear dependence of the VSGS efficiency on rotation speed.

Table 3-3 supplies the VSGS power and efficiency measurements in a tabular format. The table shows the individual component efficiencies, η_{DFG} and η_{USRC}, as well as the total generator system efficiency, η_{VSGS}. The component and system efficiencies were calculated using Equations 3-2 through 3-4, and inspection of the tabulated values shows that total VSGS efficiency is not derived from a simple product of the component efficiencies.

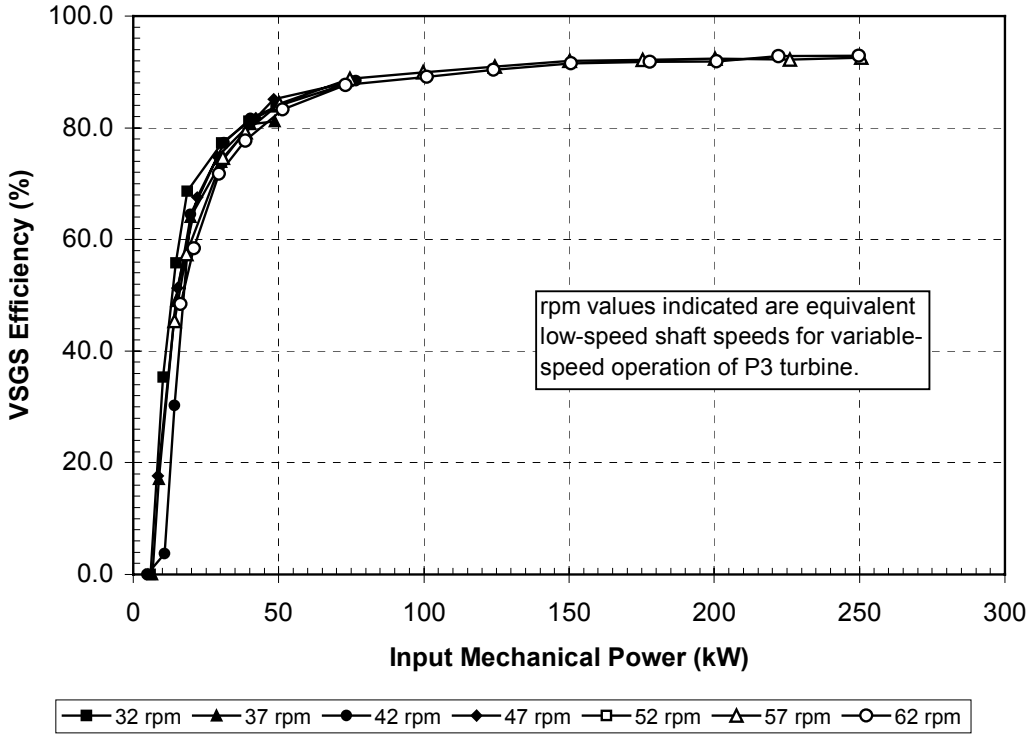

Figure 3-3. Measured VSGS efficiencies

Table 3-3. Measured VSGS Component and System Efficiencies

rpm	P_{Mech} (kW)	P_{Stator} (kW)	P_{Rotor} (V)	P_{Grid} (kW)	η_{DFG}	η_{USRC}	η_{VSGS}
836	5.8	5.1	-3.2	-0.9	32.8	53.3	0.0
838	10.2	11.5	-5.1	3.6	62.7	64.6	35.3
835	14.7	18.0	-7.2	8.2	73.5	73.5	55.8
836	18.5	24.7	-9.2	12.7	83.8	76.7	68.6
836	30.4	40.6	-14.2	23.5	86.8	83.0	77.3
836	39.8	53.8	-18.4	32.3	88.9	85.6	81.2
836	49.1	67.0	-22.6	41.1	90.4	87.3	83.7
965	6.5	5.0	-2.4	-0.4	40.0	44.4	0.0
964	8.8	8.2	-3.0	1.5	59.1	44.8	17.0
964	14.7	14.9	-4.4	7.2	71.4	57.1	49.0
966	19.7	21.4	-5.8	12.6	79.2	65.9	64.0
966	30.2	34.1	-8.4	22.3	85.1	71.2	73.8
965	40.3	47.2	-11.2	32.5	89.3	76.2	80.6
965	48.7	57.1	-13.3	39.5	89.9	75.6	81.1
1,096	4.7	1.7	-1.7	-3.8	0.0	30.9	0.0
1,096	10.7	8.3	-2.4	0.4	55.1	30.4	3.7
1,095	14.2	11.6	-2.9	4.3	61.3	39.7	30.3
1,096	19.7	18.1	-2.5	12.7	79.2	46.3	64.5
1,097	31.3	30.9	-3.1	24.2	88.8	46.3	77.3
1,097	40.4	40.8	-4.2	33.0	90.6	53.8	81.7
1,095	49.5	50.6	-5.1	41.5	91.9	56.0	83.8
1,096	76.7	80.4	-7.1	67.8	95.6	56.3	88.4
1,225	8.5	5.0	-0.5	1.5	52.9	14.3	17.6
1,225	15.2	11.5	-0.5	7.8	72.4	13.5	51.3
1,226	21.9	18.0	-0.6	14.8	79.5	18.8	67.6
1,225	29.0	24.8	-0.6	21.7	83.4	19.4	74.8
1,225	42.2	37.5	-0.5	34.5	87.7	16.7	81.8
1,225	48.3	44.2	-0.4	41.1	90.7	12.9	85.1
1,226	75.5	70.3	-0.2	66.7	92.8	5.6	88.3
1,358	9.8	5.1	0.1	2.3	53.1	0.0	23.5
1,358	16.7	11.6	0.4	9.7	71.9	0.0	58.1
1,358	21.2	14.9	1.1	13.2	75.5	0.0	62.3
1,358	28.3	21.4	1.8	20.4	82.0	0.0	72.1
1,360	38.5	31.0	2.5	31.7	87.0	28.0	82.3
1,360	50.0	40.9	4.0	42.9	89.8	50.0	85.8
1,359	76.0	63.8	5.9	68.1	91.7	72.9	89.6
1,360	99.3	83.5	8.3	89.3	92.4	69.9	89.9
1,356	125.9	105.9	12.8	114.4	94.3	66.4	90.9
1,357	147.9	125.4	13.4	135.2	93.8	73.1	91.4
1,356	174.6	148.4	15.6	160.4	93.9	76.9	91.9

Table 3-3. Measured VSGS Component and System Efficiencies (concluded)

rpm	P_{Mech} (kW)	P_{Stator} (kW)	P_{Rotor} (V)	P_{Grid} (kW)	η_{DFG}	η_{USRC}	η_{VSGS}
1,487	14.1	7.5	1.5	6.4	63.8	0.0	45.4
1,487	18.3	10.8	2.3	10.5	71.6	0.0	57.4
1,488	30.8	20.7	4.6	23.0	82.1	50.0	74.7
1,487	38.5	26.9	6.0	30.5	85.5	60.0	79.2
1,486	50.3	36.9	8.3	42.4	89.9	66.3	84.3
1,486	74.5	56.4	12.8	66.1	92.9	75.8	88.7
1,485	99.7	76.3	17.3	89.7	93.9	77.5	90.0
1,486	124.5	96.0	21.7	113.2	94.5	79.3	90.9
1,487	150.1	116.1	26.2	138.0	94.8	83.6	91.9
1,487	175.3	135.8	30.6	161.5	94.9	84.0	92.1
1,489	200.3	155.6	34.8	185.0	95.1	84.5	92.4
1,489	225.9	175.3	39.0	208.4	94.9	84.9	92.3
1,487	250.5	195.2	43.1	231.9	95.1	85.2	92.6
1,616	16.3	7.9	2.5	7.9	63.8	0.0	48.5
1,615	20.9	11.2	3.7	12.2	71.3	27.0	58.4
1,615	29.4	17.8	5.9	21.1	80.6	55.9	71.8
1,614	38.6	24.4	8.2	30.0	84.5	68.3	77.7
1,616	51.4	34.1	11.5	42.8	88.7	75.7	83.3
1,617	73.1	50.2	16.9	64.1	91.8	82.2	87.7
1,616	101.0	70.0	23.5	90.0	92.6	85.1	89.1
1,616	123.9	86.6	29.1	112.0	93.4	87.3	90.4
1,615	150.6	106.4	35.6	137.9	94.3	88.5	91.6
1,616	177.8	126.0	42.0	163.2	94.5	88.6	91.8
1,617	200.7	142.6	47.3	184.4	94.6	88.4	91.9
1,620	222.1	158.9	52.8	206.2	95.3	89.6	92.8
1,618	249.8	178.8	59.2	232.1	95.3	90.0	92.9

3.5.2 Fixed-Speed Induction Generator

Figure 3-4 shows the measured efficiency of the P3 induction generator at nominal fixed speed. When comparing Figure 3-3 with Figure 3-4, we can see that that the induction generator efficiencies are higher than those for the VSGS. Table 3-4 presents the induction generator power measurements and efficiencies in a tabular format, where the adjustment in shaft speed to approximate the generator slip is evident in the schedule of shaft speeds tested.

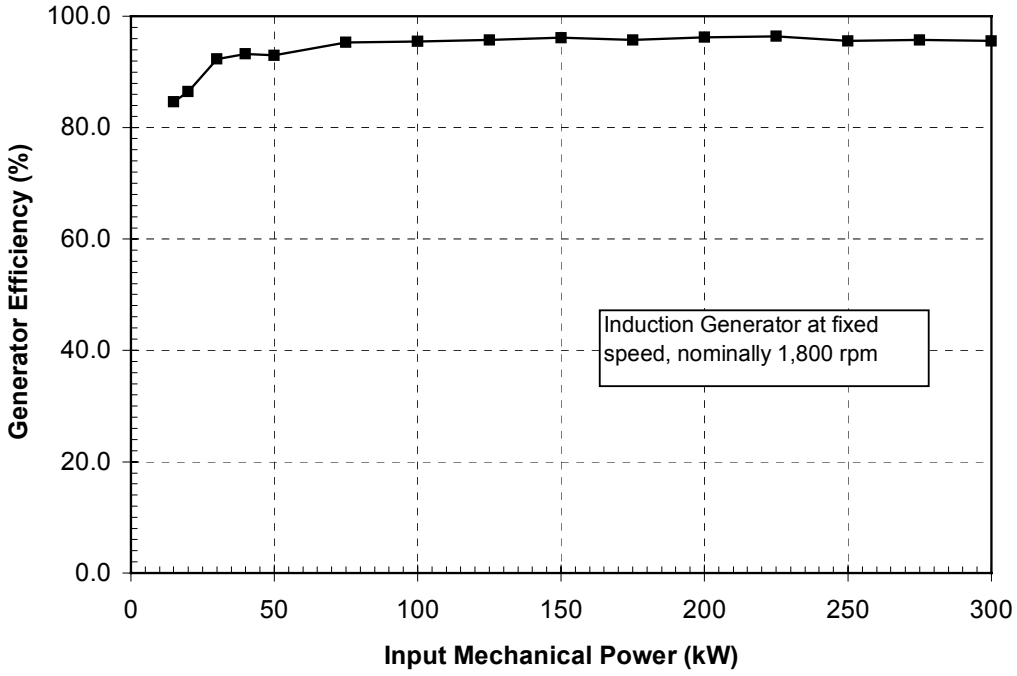

Figure 3-4. Measured efficiency for the induction generator at fixed speed

Table 3-4. Measured Power and Efficiency for the Induction Generator

HS Shaft (rpm)	Torque (ft lb)	P_{Mech} (kW)	P_{Grid} (kW)	η Elect. Sys. (%)
1,800	58.7	15.0	12.7	84.7
1,801	78.2	20.0	17.3	86.5
1,802	117.2	30.0	27.7	92.3
1,802	156.3	40.0	37.3	93.3
1,803	195.2	50.0	46.5	93.0
1,804	292.7	75.0	71.5	95.3
1,806	389.8	100.0	95.5	95.5
1,807	487.0	125.0	119.7	95.8
1,809	583.8	150.0	144.2	96.1
1,810	680.7	175.0	167.6	95.8
1,811	777.5	200.0	192.5	96.3
1,813	873.7	225.0	217.0	96.4
1,815	969.7	250.0	238.9	95.6
1,817	1065.5	275.0	263.3	95.7
1,819	1161.1	300.0	286.6	95.5

4. Analysis of System Efficiencies

In this section, we present some methods for analyzing and applying the measured efficiencies. In addition, we compare the total fixed-speed and variable-speed drivetrain efficiencies for a specific schedule of speed and shaft power. These analyses and comparisons are for illustrative purposes only. We have included a complete set of tabular data to allow interested parties to derive their own analysis method or apply the results to the analysis of alternate turbine designs.

For engineering analyses, the most convenient form of drivetrain efficiency data depends on the intended use. In some cases, the rotor power may be calculated (i.e., from an aerodynamic performance code), and an adjustment to system power is desired. In other cases, the system power may be known (i.e., from measured power performance), and the rotor power characteristics are desired. The tabular data presented here would allow the drivetrain efficiencies to be calculated in either direction of power flow. For the remaining analyses, we have adjusted the power flow to be from the low-speed shaft (rotor) toward the generator.

4.1 Curve Fits to Efficiency Data

As we discussed in Section 2.5.2, the measured gearbox efficiencies showed strong dependence on both rotation speed and power level. For this reason, power flow analyses require either an assumed or a known relationship between power and rotation speed. At each operational point, the gearbox efficiency can be calculated by a two-part lookup (i.e., interpolation) on the tabular efficiency data. As an alternative, the tabular data may be used to derive analytic expressions for the losses or efficiencies. The power loss curves of Figure 2-9 are well suited to a linear curve fit. Heine assessed candidate methods for fitting of efficiency curves, and concluded that a hyperbolic curve-fit provided a good combination of accuracy and computational simplicity (June 1998b). The hyperbolic form is:

$$\eta = C_1 - \left(\frac{C_2}{P_{in}} \right) \qquad \text{(Eqn. 4-1)}$$

where

η ≡ efficiency of the component under consideration (%)

C_1, C_2 ≡ curve-fit coefficients

P_{in} ≡ input power to component (kW).

We applied the method of Equation 4-1 to the family of efficiency curves measured for the Mark III gearbox (see Figure 2-10). Figure 4-1 shows the resulting fit to the measurements, with the corresponding curve-fit coefficients listed in Table 4-1. Note that a truncated range of efficiencies (60% to 100%) is given in Figure 4-1, so that the quality of the curve fits may be seen more easily. We can see from the figure that the hyperbolic form provides a good fit to the experimental data. However, when using equations of this form, each curve will necessarily have a lower-bound of application, such that negative efficiencies are not calculated. We derived similar hyperbolic curve fits for the induction generator and VSGS system efficiencies, shown in Figures 4-2 and 4-3, respectively.

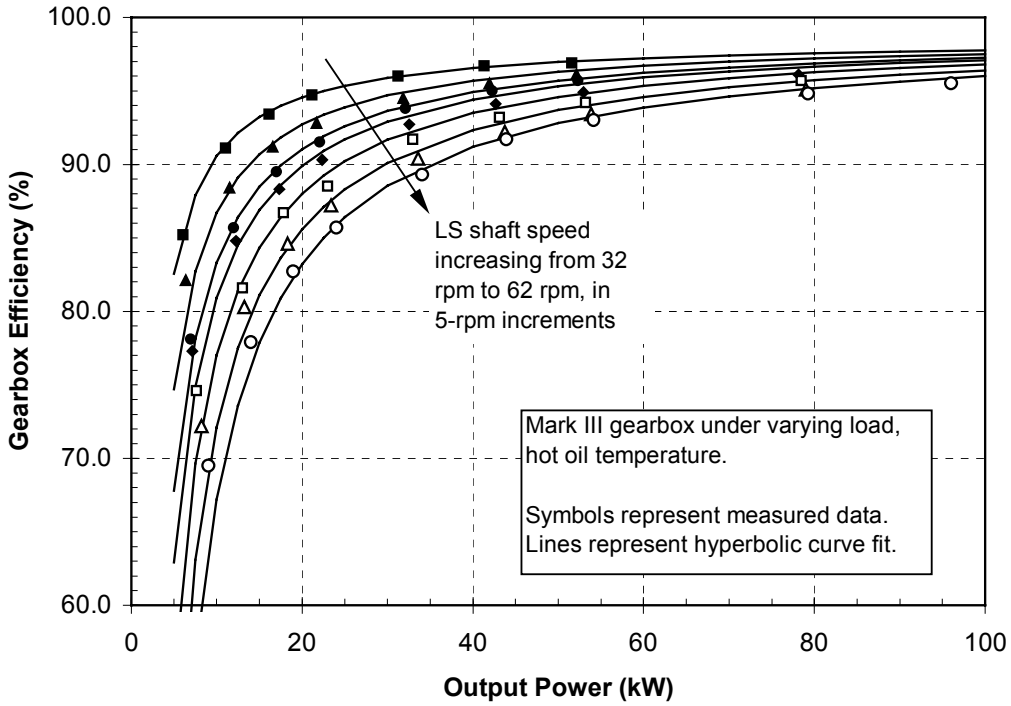

Figure 4-1. Measured Mark III efficiencies with hyperbolic curve fit

Table 4-1. Curve-Fit Coefficients used for Efficiency Curves of Figure 4-1

LS Rotation (rpm)	C_1	C_2
32	98.6	80
37	98.7	210
42	98.8	150
47	98.9	180
52	99.0	220
57	99.1	270
62	99.2	320

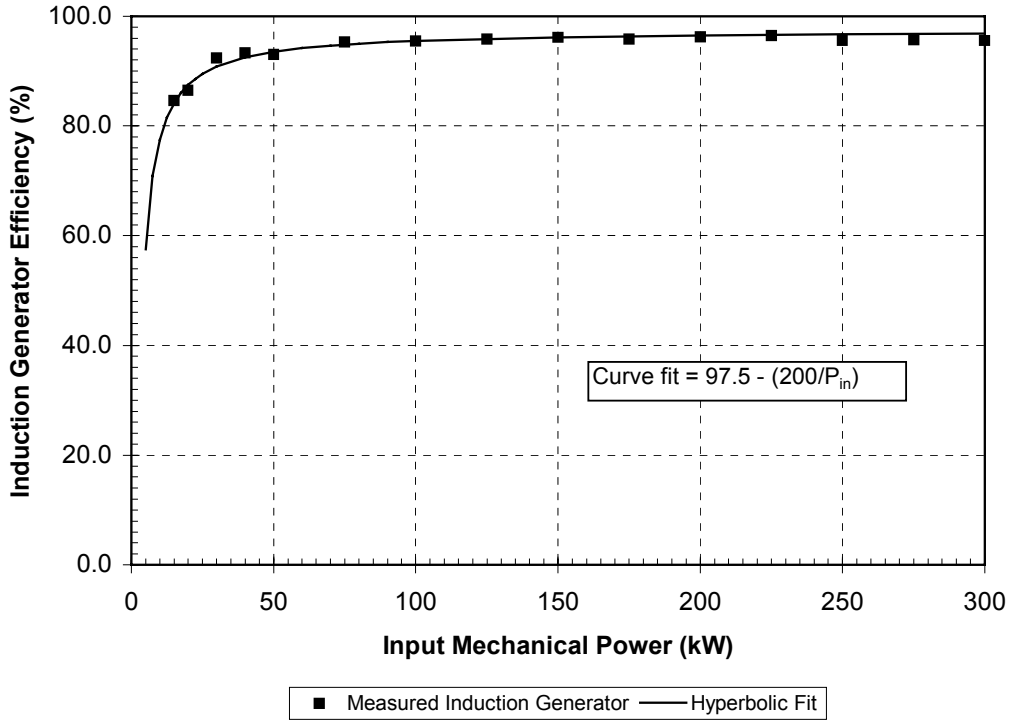

Figure 4-2. Hyperbolic curve fit for induction generator efficiencies

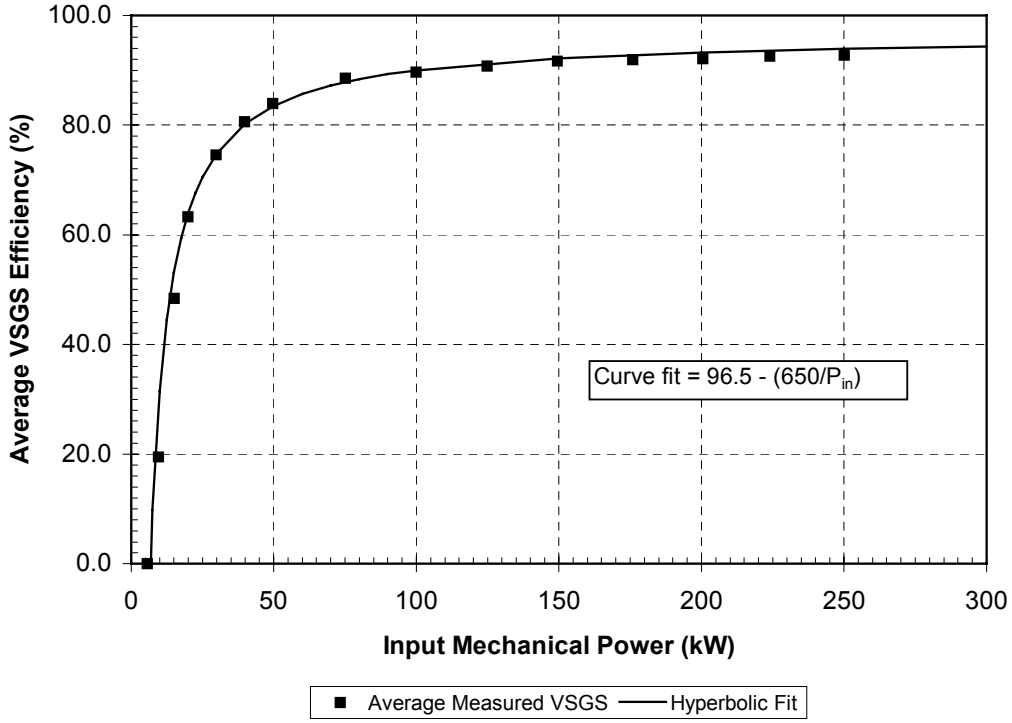

Figure 4-3. Hyperbolic curve fit for average VSGS efficiencies

4.2 Comparison of Fixed-Speed and Variable-Speed System Efficiencies

Comparing fixed-speed and variable-speed system efficiencies requires that we assume or know the relationship between shaft speed and power (for the variable-speed system). The comparisons presented here use parameters that are representative of the AWT-26 turbine to derive the power-speed relationship. This example is for illustrative purposes only, and for this reason we have taken some simplifying steps. Weigand, Lauw and Marckx (2000) provide a more detailed evaluation of the AWT-26 power performance, both predicted and measured, in both fixed-speed and variable-speed operation.

For the present example, the power-speed relationship assumes $TSR_{Design} = 8$, $C_{Pmax} = 0.5$, and $\rho = 1.225$, where:

TSR_{Design} ≡ tip-speed ratio at maximum rotor power coefficient,

C_{Pmax} ≡ maximum rotor power coefficient, and

ρ ≡ air density (kg/m^3).

Figure 4-4 shows the calculated gearbox efficiency curves. Because of the improved efficiency at low rotation speeds, the variable-speed gearbox has higher efficiencies than those for fixed-speed operation, particularly at low power levels. Figure 4-5 illustrates that the fixed-speed induction generator has higher efficiencies than the VSGS at all power levels. Figure 4-6 compares the total drivetrain efficiencies for the fixed-speed and variable-speed systems. We can see that the gearbox efficiency gains from variable-speed operation do not entirely offset the additional losses of the VSGS, and as a result, the fixed-speed drivetrain efficiencies are higher than those for the variable-speed drivetrain.

Note that a lower total drivetrain efficiency does not necessarily imply lower power performance for variable-speed operation of a turbine, because the variable-speed turbine can be controlled in a way that maximizes the rotor power available. Additionally, the total impact on turbine cost of energy requires a complete system evaluation, including power performance, mean drivetrain torque levels, torque transients, and noise considerations. The work of Weigand, Lauw, and Marckx (2000) addresses these issues more completely.

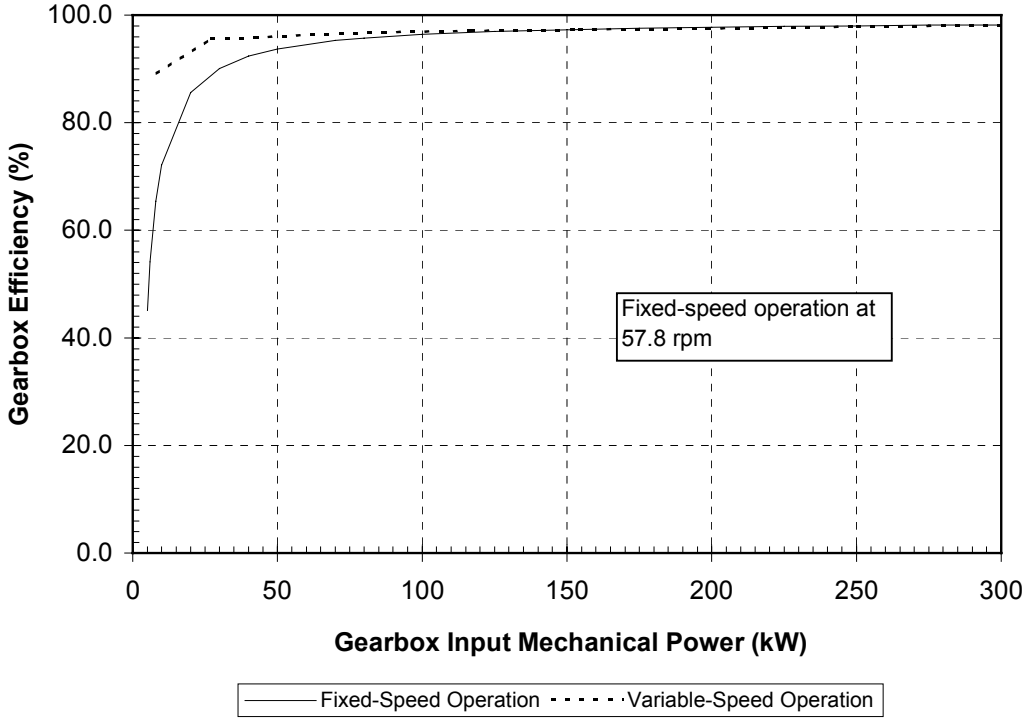

Figure 4-4. Comparison of fixed-speed and variable-speed gearbox efficiencies

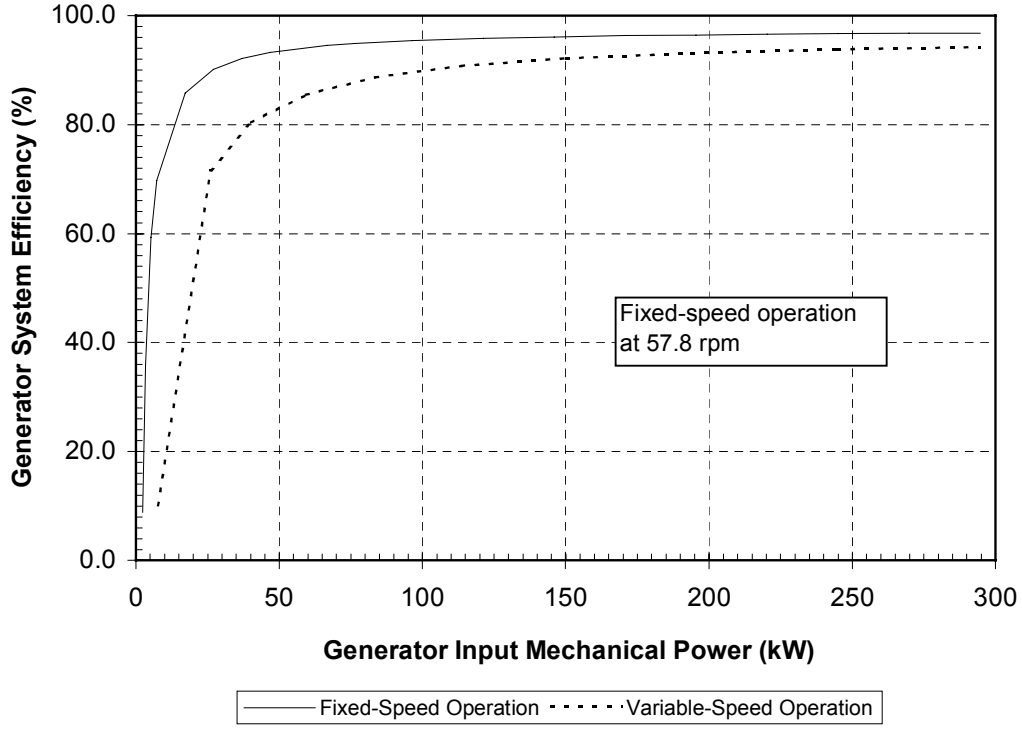

Figure 4-5. Comparison of fixed-speed and variable-speed generator system efficiencies

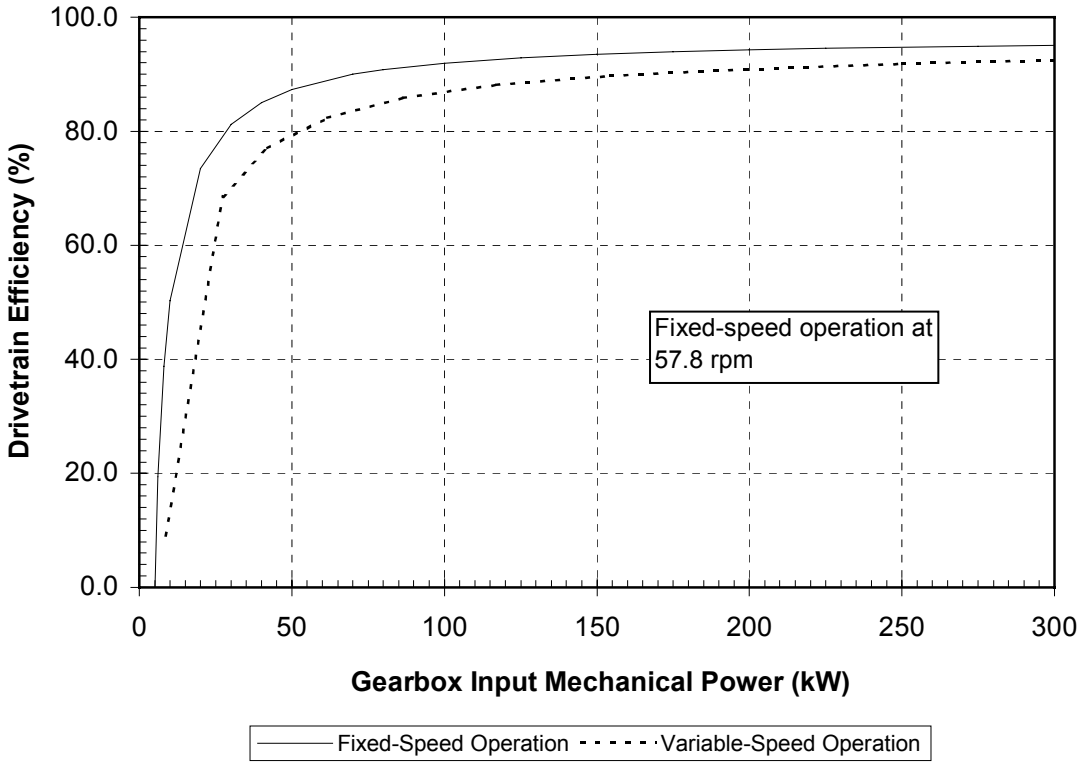

Figure 4-6. Comparison of fixed-speed and variable-speed drivetrain efficiencies

5. Conclusions

EPC and AWT performed laboratory tests of drivetrain component efficiencies, both for the fixed-speed P3 turbine and the EPC variable-speed retrofit.

The AWT gearbox tests involved three different models of Flender PZBS-170 (two-stage, planetary) gearboxes. The test results showed that the gearbox power losses resulted primarily from oil churning, depended strongly on oil temperature, increased rapidly with shaft rotation speed, and increased weakly with gearbox load. At a given (low-speed shaft) rotational speed, the power losses were found to be independent of both gearing ratio and rotation direction.

EPC laboratory testing included both the original P3 induction generator at fixed speed, and the DFG / power converter VSGS system that EPC designed for variable-speed operation of P3. The fixed-speed induction generator had higher efficiencies than the VSGS at all power levels.

In this report, we presented methods for analyzing and applying the measured drivetrain efficiencies, and compared the fixed-speed and variable-speed drivetrain efficiencies. We included a set of hyperbolic curves to provide an accurate and convenient fit to the measured efficiencies.

To develop an illustrative comparison of component and drivetrain efficiencies, we used AWT-26 operational parameters. Because of the improved efficiency at low rotation speeds, the variable-speed gearbox has higher efficiencies than those seen during fixed-speed operation, particularly at low power levels. In contrast, the fixed-speed induction generator has higher efficiencies than the VSGS at all power levels. Evaluation of the total drivetrain shows that the gearbox efficiency gains from variable-speed operation do not offset the additional losses of the VSGS, and as a result, the fixed-speed drivetrain efficiencies are higher than those for the variable-speed drivetrain.

6. References

1. Weigand, C.H.; Lauw, H.K.; Marckx, D.A. (November 2000) *Variable-Speed Generation Subsystem using the Doubly Fed Generator*. NREL/SR-500-27066. Golden, Colorado: National Renewable Energy Laboratory.
2. Advanced Wind Turbines, Inc. (February 1996). *AWT-26/57 Gearbox Efficiency Test Report, TR270001*, Seattle, Washington.
3. McVittie, D. (May 8, 1997). Telephone conversation with AWT engineers about loss mechanisms for test gearboxes.
4. Heine, G. (June 1998a). Spreadsheet calculations to evaluate the effect of assuming equal losses in test gearboxes.
5. Heine, G. (June 1998b). Spreadsheet calculations to evaluate the hyperbolic curve-fits to component efficiency data.

REPORT DOCUMENTATION PAGE

Form Approved
OMB NO. 0704-0188

1. AGENCY USE ONLY (Leave blank)	2. REPORT DATE	3. REPORT TYPE AND DATES COVERED
	January 2002	Subcontract; November 4, 1997—November 3, 2000

4. TITLE AND SUBTITLE
Laboratory Testing of Drivetrain Component Efficiencies for Constant-Speed and Variable-Speed Wind Turbines

5. FUNDING NUMBERS
WER12410
TAM-8-17228-01

6. AUTHOR(S)
Global Energy Concepts, L.L.C.

7. PERFORMING ORGANIZATION NAME(S) AND ADDRESS(ES)
Global Energy Concepts, L.L.C.
5729 Lakeview Drive NE, #100
Kirkland, WA 98033

8. PERFORMING ORGANIZATION REPORT NUMBER

9. SPONSORING/MONITORING AGENCY NAME(S) AND ADDRESS(ES)
National Renewable Energy Laboratory
1617 Cole Blvd.
Golden, CO 80401-3393

10. SPONSORING/MONITORING AGENCY REPORT NUMBER
NREL/SR-500-30117

11. SUPPLEMENTARY NOTES
NREL Technical Monitor: Paul Migliore

12a. DISTRIBUTION/AVAILABILITY STATEMENT
National Technical Information Service
U.S. Department of Commerce
5285 Port Royal Road
Springfield, VA 22161

12b. DISTRIBUTION CODE

13. ABSTRACT *(Maximum 200 words)*

Under a subcontract with the National Renewable Energy Laboratory, Electronic Power Conditioning, Inc., (EPC) designed, built, and tested variable-speed generator systems (VSGS) as retrofits for two different existing fixed-speed turbine designs. The VSGS were tested in the laboratory and in the field. EPC lab testing included both the original P3 induction generator at fixed speed and the doubly-fed generator / power converter VSGS system that EPC designed for variable-speed operation of P3. The fixed-speed induction generator had higher efficiency than the VSGS at all power levels.

14. SUBJECT TERMS
drivetrain component efficiency; constant-speed wind turbines; variable-speed wind turbines; wind technology; turbine retrofits

15. NUMBER OF PAGES:

16. PRICE CODE

17. SECURITY CLASSIFICATION OF REPORT	18. SECURITY CLASSIFICATION OF THIS PAGE	19. SECURITY CLASSIFICATION OF ABSTRACT	20. LIMITATION OF ABSTRACT
Unclassified	Unclassified	Unclassified	UL